

ASSESSMENT OF LOW TEMPERATURE ELECTRICITY PRODUCTION WITH FOCUS ON GEOTHERMAL ENERGY

Master's Thesis within the Sustainable Energy Systems programme

ANDREAS SCHEYHING

Department of Energy and Environment
Division of Heat and Power Technology
CHALMERS UNIVERSITY OF TECHNOLOGY
Göteborg, Sweden 2012

MASTER'S THESIS

Master's Thesis within the *Sustainable Energy Systems* programme

ANDREAS SCHEYHING

SUPERVISORS:

Mathias Gourdon, Sven Wellsandt

EXAMINER

Mathias Gourdon

Department of Energy and Environment
Division of Heat and Power Technology
CHALMERS UNIVERSITY OF TECHNOLOGY
Göteborg, Sweden 2012

ASSESSMENT OF LOW TEMPERATURE ELECTRICITY PRODUCTION WITH
FOCUS ON GEOTHERMAL ENERGY

Master's Thesis within the *Sustainable Energy Systems* programme
ANDREAS SCHEYHING

© ANDREAS SCHEYHING, 2012

Department of Energy and Environment
Division of Heat and Power Technology
Chalmers University of Technology
SE-412 96 Göteborg
Sweden
Telephone: + 46 (0)31-772 1000

Cover:
Schematic drawing of the RORC, © Andreas Scheyhing

Chalmers Reproservice
Göteborg, Sweden 2012

ASSESSMENT OF LOW TEMPERATURE ELECTRICITY PRODUCTION WITH FOCUS ON GEOTHERMAL ENERGY

Master's Thesis in the *Sustainable Energy Systems* programme

ANDREAS SCHEYHING

Department of Energy and Environment

Division of Heat and Power Technology

Chalmers University of Technology

ABSTRACT

With the rise of environmental awareness and increased electricity prices, low temperature electricity production cycles are getting more and more into focus. These include applications that produce electricity from industrial waste heat, which otherwise would have been released to the environment. They can also be used for medium enthalpy geothermal heat sources from 125 to 225 °C. The purpose of this Master Thesis is to identify and compare different technologies to produce low temperature electricity, according to their profitability and efficiency. Moreover, this Thesis focuses on investigating electricity cycles for further use in geothermal power plant applications. Finally the specific case of Geotermica¹ is studied.

Low temperature electricity production cycles have been identified during a literature research. Based on that, the most promising cycles have been analysed in detail. These are the ORC (Organic Rankine Cycle), RORC (Regenerative Organic Rankine Cycle) and the LTD (Low Temperature Differential) Stirling engine. The analysis is carried out in Aspen + and with a modified Schmidt formula for the LTD Stirling engine according to Chen (2003). Starting with set boundaries, each cycle is researched in costume cases while varying the same heat source and sink. The LTD Stirling engine shows the best performance with 18.2% system efficiency. The simulated LTD Stirling engine, however, has a temperature limitation of 150°C and cannot be used above this temperature. For higher temperatures, up to 185°C, the highest efficiency was obtained with the RORC of 18.5%.

In the Geotermica case, the LTD Stirling engine did not take part, due to missing economic data in the literature. With the expected well flows of the planned geothermal power station in the south of Italy on the Aeolian Islands and the local weather data, the RORC is most promising. The economic evaluation of the ORC and the RORC show as well, that the RORC is the most profitable, although it is the more expensive one with an investment cost of 10.2 Mio. € whereas the ORC costs 8.9 Mio. €. The RORC has an annual income of 6.3 Mio. € which is roughly 1 Mio. € more than the ORC. Together with the exploration and drilling costs of 30 Mio. €, the payback time is estimated to 6.4 years.

¹ Geotermica is the company who plans to build the analysed geothermal power station in south Italy.

Key words: ORC, RORC, LTD Stirling engine, geothermal, electricity

Contents

ABSTRACT	I
CONTENTS	III
PREFACE	V
NOTATIONS	VII
1 INTRODUCTION	1
1.1 Objective	1
1.2 Limitations and Assumption	2
1.3 Method	2
2 GEOTHERMAL ELECTRICITY PRODUCTION	3
2.1 Europe and Worldwide	3
2.2 Environmental impact	3
3 LITERATURE REVIEW	5
3.1 Technologies	5
3.2 Technologies of interest	8
4 LOW TEMPERATURE ELECTRICITY PRODUCTION CYCLES	9
4.1 Organic Rankine Cycle	9
4.1.1 Working fluid	9
4.1.2 Design of the ORC	10
4.2 Regenerative Organic Rankine Cycle	13
4.2.1 Working fluid	13
4.2.2 Design of the RORC	13
4.3 Stirling engine	16
4.3.1 Design of the LTD Stirling engine in the gamma configuration	17
4.3.2 Modelling the LTD Stirling engine	18
5 SIMULATION	21
5.1.1 Assumptions common to all technologies	21
5.1.2 Investigated cases	22
5.2 Simulation of the ORC	23
5.2.1 Case 1: Basic	23
5.2.2 Case 2: Superheating	25
5.2.3 Case 3: Varying Cooling	27
5.2.4 Case 4: Varying heating	29

5.3	Simulation of the RORC	30
5.3.1	Case 1: Basic	30
5.3.2	Case 2: Varying feed organic fluid pressure	31
5.3.3	Case 3: Varying cooling	32
5.3.4	Case 4: Varying heating	33
5.4	Simulation LTD Stirling engine	34
5.4.1	Case 1: Basic	34
5.4.2	Case 2: Varying cooling	34
5.4.3	Case 3: Varying heating	35
6	ECONOMICS	37
7	GEOTERMICA	39
7.1	Technical analysis	39
7.2	Economic analysis	40
8	RESULTS AND DISCUSSION	43
8.1	Comments on the assumptions	43
8.2	ORC / RORC	44
8.3	LTD Stirling engine	45
8.4	Economics	46
8.5	Geotermica	46
9	CONCLUSIONS	47
10	REFERENCES	49
	APPENDIX 1	53
	APPENDIX 2	55
	APPENDIX 3	57
	APPENDIX 4	59

Preface

In this Master's Thesis, a techno-economic analysis of low temperature electricity production cycles has been carried out at the Division of Heat and Power Technology, Chalmers University of Technology. The aim was to identify the best techno-economic solution, to produce electricity from low temperature heat sources. Further a specific case for the company Geotermica AB has been analysed.

I would like to express my gratitude to my supervisors, Mathias Gourdon and Sven Wellsandt for their support and I highly appreciated them for their patience. I also want to thank Stefan Heyne and Rickard Fornell who helped me in technical problems. At last, I want to thank Guy de Caprona from Geotermica AB, who supported this Master's.

Göteborg August 2011
Andreas Scheyhing

Notations

Symbol

A	Area	m^2
c_p	Specific heat capacity	$\text{kJ}/(\text{kgK})$
CED	Chemical Engineering Design	-
$EGEC$	European Geothermal Energy Council	-
EU	European Union	-
F	Correction factor	-
G	Generator	-
GEA	United States Geothermal Energy Association	-
h	Enthalpy	kJ/kg
$ISBL$	Inside battery limits	-
LTD	Low temperature differential	-
m	Mass	kg
\dot{m}	Mass flow	kg/s
n	Engine speed	$1/\text{min}$
ORC	Organic Rankine cycle	-
$OSBL$	Off-site battery limits	-
P	Power	W
p	Pressure	bar
p_m	Mean pressure	kPa
PDE	Plant Design and Economics for C. E.	-
\dot{Q}	Specific heat duty	kW
R	Universal gas constant	$\text{Nm}/(\text{kgK})$
$RORC$	Regenerative Organic Rankine cycle	-
s	Entropy	$\text{kJ}/(\text{kgK})$
T	Temperature	$^{\circ}\text{C}$
V	Volume	dm^3
\dot{W}	Specific work	kW
X	Fraction	-
α	Phase angle	$^{\circ}$
β	Volume expansion coefficient	$1/\text{K}$
ε	Compression ratio	-
η	Efficiency	$\%$
φ	Rotation angle	$^{\circ}$

Indices

air	Air
Ar	Work
Bew	Moving
C	Carnot
CF	Carnot-Factor
$cool$	Cooling
con	Condenser
cr	Critical

<i>cycle</i>	Cycle
<i>eva</i>	Evaporator
<i>Geo</i>	Geothermal
<i>H</i>	Hot side
<i>HP</i>	High pressure
<i>I</i>	Thermal system efficiency
<i>in</i>	In
<i>K</i>	Cold side
<i>LP</i>	Low pressure
<i>min</i>	Minimum
<i>max</i>	Maximum
<i>net</i>	Network
<i>ORC</i>	Organic Rankine cycle
<i>out</i>	Out
<i>p</i>	Pump
<i>R</i>	Regenerator
<i>RORC</i>	Regenerative Organic Rankine cycle
<i>Sch</i>	Schmidt
<i>t</i>	Turbine
<i>T</i>	Deadspace
<i>V</i>	Volume
<i>w</i>	Water

1 Introduction

Since a range of environmental impacts of global warming took place, such as rising sea level, changed seasons, melting glaciers and pol caps, greenhouse gases became a hot topic within the public and the governments. To stop this trend, the EU Heads of State and Government enacted the “20-20-20” targets which should be achieved by 2020. The first target is the reduction of greenhouse gas emissions by 20% below 1990 levels. The second is to increase the renewable energy production up to 20%. Last but not least, the last target is to reduce the primary energy usage with 20% by improving the energy efficiency (European Commission, 2010).

So what possibilities are there to decrease the carbon dioxide footprint and to increase the efficiency in the electricity production sector?

On the one hand, raising the efficiency of power stations and industrial factories gives an opportunity for decreasing the fuel demand and increasing the power output which would lead to reduce specific CO₂-emissions. These opportunities can include using low temperature heat sources, otherwise wasted, to produce electricity by using low temperature electricity production cycles. A Cooling demand is available in almost all industrial processes, such as in oil refining or steel casting and also in power plants. Additional usage of low temperature electricity cycles in different processes could also decrease the production cost of the equipment. As a consequence thereof, the investment cost for waste heat electricity or geothermal plant will decrease, which could help to further disseminate low temperature electricity production and lower the carbon dioxide emissions.

Geothermal enthalpy resources are generally classified by temperature. The medium temperature level ranges from 125°C to 225°C, below and above this range, the sources are labelled as low and high respectively (Hochstein, 1990). Compared to the temperature used for conventional electricity production, these temperatures are, however, very low. Subsequently, this Master Thesis deals with low temperature electricity production.

This Master’s Thesis is performed in collaboration with Alpha Solutions and Geotermica AB. Alpha Solutions is a consultant specialized in heat transfer and fluid dynamics. Geotermica AB is a Swedish company, researching environmentally friendly geothermal power generation and district heating possibilities all over Europe.

1.1 Objective

The objective of this Master’s Thesis is to identify and compare different technologies to produce low temperature electricity, according to their profitability and efficiency. Moreover, this thesis work will focus on investigating electricity cycles for use in geothermal power plant applications and, finally, the specific case of Geotermica will be studied.

1.2 Limitations and Assumption

In this thesis project, literature based data is validated and as far as possible tested with simulation tools. The thesis does not aim on improving the different power production cycles as such, nor will any experimental validation be performed. Moreover, a sensitivity analysis is performed for the different power production cycles, in which some, but not all parameters are researched. The limitation lies as well on the simulation tool and on the calculation method / equations being used. Simulation tools try to replicate the reality and need to be validated experimentally.

1.3 Method

Based on a literature review, different cycles are identified and investigated. The systems are modelled and compared to each other using the same system boundaries, conditions and properties, such as heat and cooling source. This is done by Aspen +, a process simulation tool mainly used in the Oil & Gas industry and with thermodynamic equations. Further an economic evaluation is performed according to investment data that can be found in literature. Last but not least, the specific case of Geotermica AB is evaluated and analysed and project costs estimated.

The first step is to identify possible technologies that are available in the temperature range from 125°C up to 225°C. This task is accomplished by a literature review.

The next step uses Aspen + to model and evaluate the low temperature electricity cycles that were previously investigated, as far as possible. Low temperature electricity cycles, that cannot be modelled in Aspen +, will be evaluated with thermodynamic equations in Excel.

The third step deals with the profitability. Dependent on the efficiency and the heat source temperature, the profits are estimated for the investigated cycles. This is done mainly with the book Chemical Engineering Design (CED) (2009) and with the book Plant Design and Economics for Chemical Engineers (PDE) (2003).

In the last step of the study, the specific case of interest for Geotermica will be investigated in detail. In that analysis the available temperatures, pressure and local properties available at a typical geothermal exploration site are used in the simulated models, as well as in the economic evaluation.

2 Geothermal electricity production

2.1 Europe and Worldwide

Geothermal energy is heat stored within the earth. In the Earth 12.6×10^{24} MJ of heat is stored while the Earth crust contains approximately 5.4×10^{21} MJ. The total energy demand worldwide per year is compared to that, very small, only 6×10^{13} MJ per year. However, only a fraction of this huge heat source can be utilized.

The first time geothermal energy was utilized, was in Larderello, Italy, in 1904. Today approximately 1 GW of geothermal electric power is in operation in the European Union (EU), producing 7 000 GWh of electricity per year, see Figure 2.1. Only a few countries in Europe actually produce electricity from geothermal sources, these are Italy, France, Portugal and Iceland. In some of the other countries in the EU, geothermal power is used for district heating. The IEA reports a constant growing rate of about 200 MW/year since 1980 until 2005. The worldwide geothermal electricity production reached in 2007 10 GW, producing 56 TWh per year (European Commission, 2011).

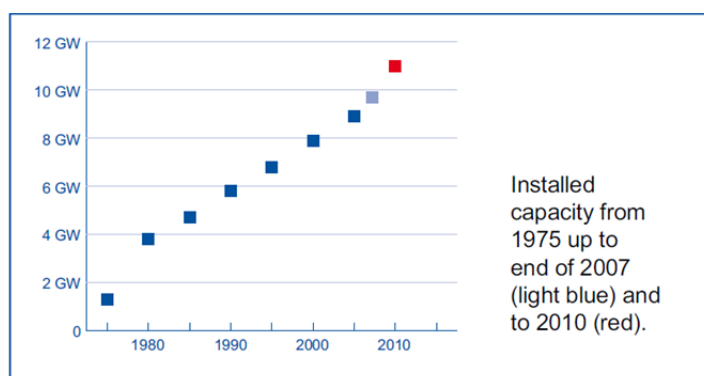


Figure 2.1 Worldwide installed geothermal power capacity, (European Geothermal Energy Council (EGEC), 2009)

Between 2005 and 2010, geothermal electricity production increased by 20%. Moreover, in 2007, there were 46 countries planning or developing geothermal power stations. In 2010, the US Geothermal Energy Association (GEA) reported an increase by 52% of countries, which are considering geothermal electricity production, since 2007. Europe and Africa are the two regions in the world where the number of projects increased the most.

2.2 Environmental impact

Using geothermal energy can have local environmental impacts. In a city of Greece, Milos, there were problems with sulphur smell in the town. When silica scale on windows was detected as well, the resistance in the local population grew. So after a short operating time of two years, the plant had to be abandoned. Another issue can be caused with the reinjection. In Basel, Switzerland, the reinjection of the brine caused several earthquakes. The earthquakes had strength of up to 3.4 on the Richter scale and nearly 2000 reports of damage have been reported. The reasons relied on

incorrectly positioned or badly drilled boreholes (European commission, 2009). Geothermal power stations do not create any CO₂ gases. It could happen, that gases from the earth are released like in the case of Milos. But those ones can be removed and is a routine procedure in geothermal power stations according to Fridleifsson (2001).

3 Literature Review

3.1 Technologies

According to the EGEC, three main types of geothermal electricity production cycles are in use worldwide. Dry steam power plants has a share of 28% of the world's geothermal electricity production, utilizes dry steam that is piped directly from the geothermal well. Flash cycles have the largest share of 64% and binary cycles, like the Organic Rankine Cycle, have the smallest share of 8%, see Figure 3.1

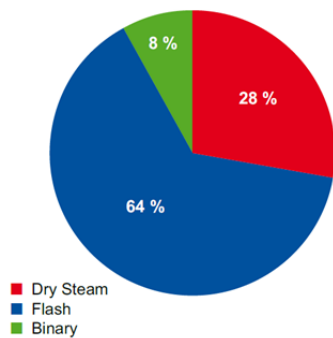


Figure 3.1 World Geothermal Power plant distribution in 2009, (EGEC, 2009)

In the literature review, different cycles have been identified for low temperature heat sources utilization. These cycles are shortly described below.

The simple organic Rankine cycle

The simple organic Rankine cycle (ORC) is seen Figure 3.2. It main equipment consists of:

- Pump
- Evaporator
- Turbine + Generator
- Condenser

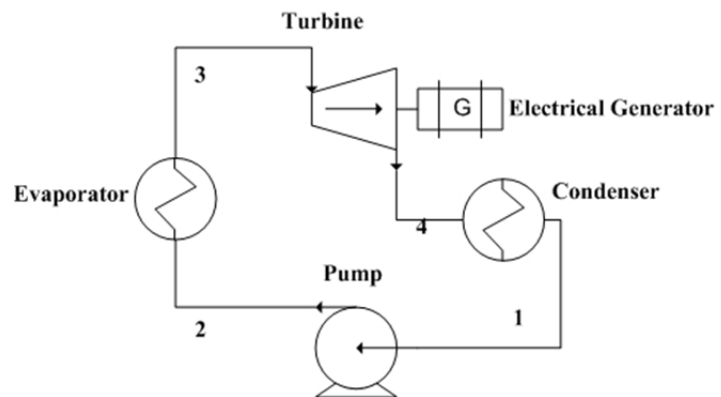


Figure 3.2 Simple organic Rankine cycle

At first the organic working fluid is evaporated in the evaporator that is driven by geothermal heat or any other low temperature heat source. The vaporized organic fluid is expanded in the turbine, which is mechanically connected to an electrical generator. After the expansion, the organic steam is condensed in the condenser. From the condenser the organic fluid is pressurized in the pump and moved back to the evaporator.

The regenerative organic Rankine cycle

The regenerative organic Rankine cycle (RORC) is based on the ORC as seen in Figure 3.3 and Figure 3.2. It consists of:

- A low and high pressure pump
- Evaporator
- Two turbines
- Feed organic heater
- Condenser

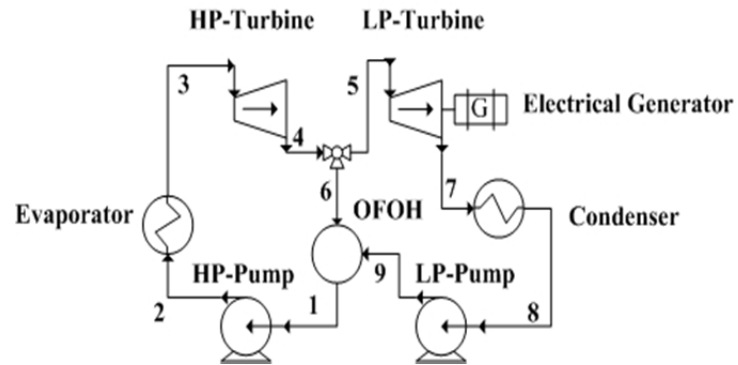


Figure 3.3 Basic components of the RORC

Vaporized organic fluid is expanded in the turbine in two stages. After the first stage, a bleed stream, feeds the open feed organic heater. The open feed organic heater pre heats the sub-cooled fluid from the low-pressure pump to saturated liquid with the feed stream. The second stage of the turbine, or the low-pressure part, expands the organic steam further. Then in the condenser the incoming organic steam is condensed. From the condenser the organic liquid is pumped from the low-pressure pump through the open feed organic heater to the high-pressure pump. After the high-pressure pump the sub cooled organic fluid is heated and evaporated in the evaporator.

The Rankine cycle with flash

The Rankine cycle with flash is seen in Figure 3.4. The cycle mainly consists of:

- Flash chambers
- High and low pressure turbine + Generator
- Condenser

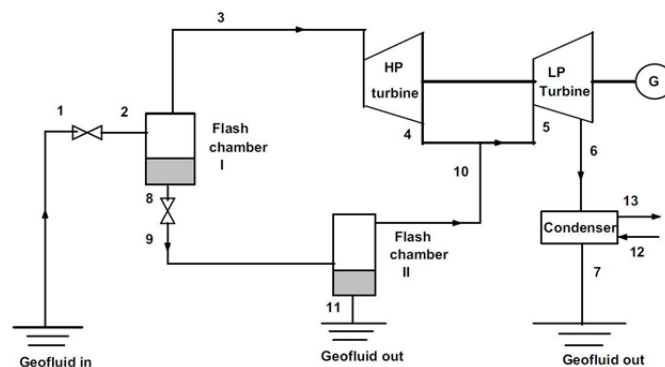


Figure 3.4 Rankine cycle with double flash (Yari, 2010)

The Rankine cycle with one or more flash chambers, are mainly used for geothermal power plants. The geo fluid from the ground is directly utilized to produce electricity. In the first step the pressure is reduced in the first flash chamber at constant enthalpy. The steam then goes through a high-pressure turbine. If the fluid temperature is high enough, a second flash chamber is installed. The liquid from the first flash chamber is

then flashed again at a lower pressure. Both streams, the first stream after the high-pressure turbine and the stream from the second flash chamber are then mixed together to feed a low-pressure turbine. From here the steam, is condensed in a condenser and re-injected to the ground.

Kalina cycle with internal heat exchanger

The Kalina cycle is a recovery cycle with non-isothermal evaporation and condensation mainly through the use of mixtures. The Kalina cycle is compared to the other cycles a very new technology. Al Kalina invented the new thermodynamic power cycle with a mixture of water and ammonia in the 1980s. (Worek, 2007) The Kalina cycle is shown in Figure 3.5. The equipment is listed below:

- Condenser
- Pump
- Regenerator
- Evaporator
- Separator
- Turbine + Generator
- Absorber

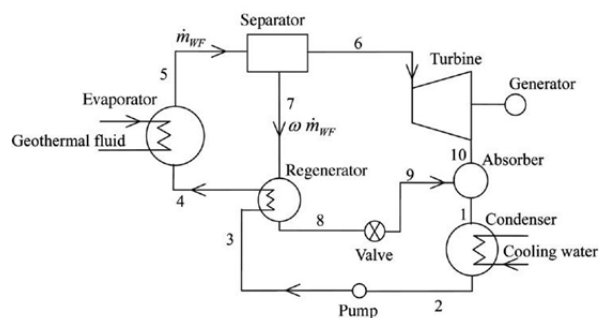


Figure 3.5 Basic components of the Kalina cycle (Worek, 2007)

The ammonia-water mixture is heated in the evaporator. In the separator it is split to a saturated rich ammonia-water vapour and lean ammonia-water mixture. The rich solution is expanded in the turbine and then mixed with the lean solution in the absorber. After condensing the mixture in the condenser, it is pressurised in the pump and pre-heated in the regenerator before entering the evaporator again.

The Stirling Engine

There are three types of the Stirling engines, alpha, beta and gamma. Later in this Master thesis, all three kinds are explained. The Stirling engine is shown in Figure 3.6. The Stirling engine consists of:

- Displacer
- Power piston
- Heater
- Regenerator
- Cooler

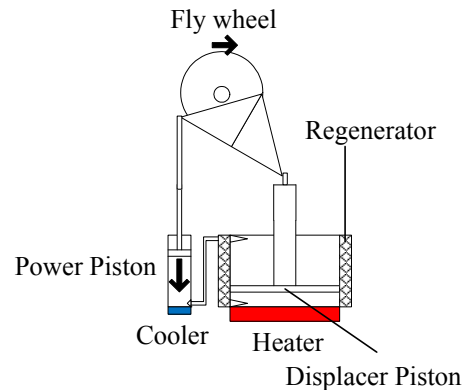


Figure 3.6 Stirling engine in the gamma configuration

The displacer and the power piston are both connected to a flywheel. The working fluid is compressed isothermally by the power piston, while the cooler removes the heat from the working fluid during compression. The working fluid is heated isochorically in the displacer by the heater. Then the working fluid is isothermally expanded in the power piston while the heater continues to heat the gas. After reaching its maximum volume in the power piston, the working fluid is pushed back by the power piston into the displacer cylinder under isochoric conditions while it passes the cooler and gets cooled.

3.2 Technologies of interest

During the literature research, different low temperature power cycles have been investigated. The simple organic Rankine cycle, the regenerative organic Rankine cycle and the LTD Stirling engine came into question, because they showed promising results. The Rankine cycle with flash was not considered, due to the complicated and expensive structure. Another reason is the temperature range. The Rankine cycle with flash usually operates at temperatures above 200°C. The Kalina cycle is not considered either, for environmental reasons. The working fluid of the Kalina cycle, ammonia, cannot be used at the geothermal power station in Italy (personal communication with G. de Caprona, Geotermica).

4 Low temperature electricity production cycles

4.1 Organic Rankine Cycle

The Organic Rankine Cycle (ORC) is in principal a Rankine cycle with one big difference, the working fluid. Instead of using water, the ORC uses an organic working fluid. The advantages of the Organic Rankine Cycle are the high thermodynamic cycle efficiency and the absence of moisture during the vapour expansion, which causes low mechanical stress to the turbine. However, the ORC has as well a disadvantage, for example the thermal stability of its organic working fluid. Depending on the organic fluid, the ORC has a maximum thermal operating range, which is much lower, than the ORC equipment is able to. Operating above the thermal stability of the organic fluid, would lead to decomposition. This could destroy the ORC equipment in the worst case. According to Turboden, a manufacturer of ORC, little and simple maintenance procedures are necessary. Currently modules from 1MW_{el} until 7MW_{el} are available. (Turboden, 2011)

4.1.1 Working fluid

The working fluids can be divided in three groups. These are the wet, dry and isentropic fluids. Wet fluids are characterized by their negative slope in the T-s diagram and are not recommended for ORC's. This is because when using a wet fluid, superheating is necessary to avoid a liquid formation during the expansion. Positive slope indicates dry fluids. Vertical saturation curves describe isentropic fluids. It is common to use dry or isentropic fluids. As the formation of liquid during the expansion is avoided, superheating is not necessary. In Summary, the risk of droplet erosion on the turbine blades is close to zero when using isentropic or dry fluids. One example of each fluid group is shown in Figure 4.1.

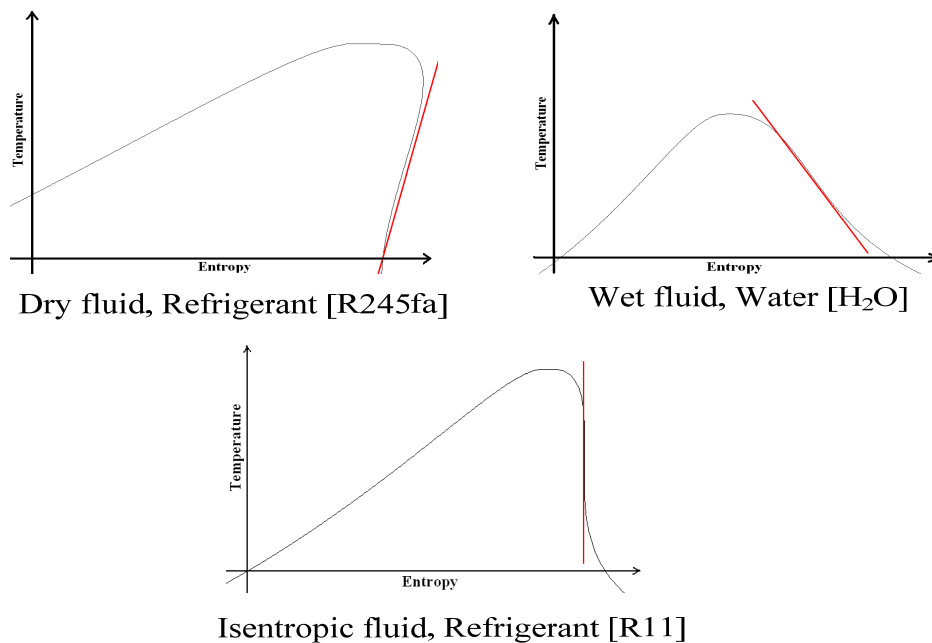


Figure 4.1 Temperature - entropy diagram for dry, wet and isentropic fluids

In the selection of working fluid, two different characteristics need to be considered at least. One is the possible environmental impact and the second is how the fluid affects the efficiency of the cycle. According to the paper of Kosmadakis (2008), the fluid that combines both these properties is R245fa, a 1,1,1,3,3-pentafluoropropane. The Ozone Depletion Potential (ODP) of R245fa is zero and the Global Warming Potential (GWP) for 20 years has a value of 3000. The ODP indicates the degradation ability per kilogram emissions compared to the emissions of R11 and GWP indicates the contribution per kilogram emission relative to CO₂ (Gourdon, 2011). The thermal stability was investigated by Angelino (2002). According to Angelino, R245fa has a magnificent thermal stability for temperatures up to 300 °C and no decomposition were detected at temperatures below that. So the first fluid tested, is R245fa. The second fluid tested is R601, n-pentane (CH₃-3(CH₂)-CH₃), which is as well a dry fluid. It contains no chlorine atoms and has therefore zero ODP and the GWP for 20 years is 3, but it is highly flammable. N-pentane was chosen, due to a higher critical temperature compared with R245fa. It is expected that a high critical fluid temperature, will influence the system efficiency. Values of the critical point of the working fluids R245fa, R601 and the geothermal water are shown in *Table 4.1*.

Table 4.1 The critical point for the different working fluids values (REFPROP, 2003)

Type	Critical temperature, T _{cr} [°C]	Critical pressure, p _{cr} [bar]
R245fa	154.05	36.4
R601	196.55	33.7
Water	373.95	220.64

4.1.2 Design of the ORC

The ORC is schematically shown in Figure 4.2 and basically consists of the same components as an ordinary water-steam Rankine cycle. In Figure 4.3 the corresponding thermodynamic states are shown.

Stage 1 to 2:

The pump creates the necessary pressure in the ORC. Saturated liquid exiting from the condenser is pressurised in the pump to a specific level at almost isothermal conditions. The required work for the pump is

$$\dot{W}_{p,net} = \eta_p \dot{m}(h_1 - h_2) \quad (4.1)$$

Stage 2 to 3:

After the pump the organic liquid will be a sub-cooled fluid. In the evaporator the working fluid is heated and evaporated. This can be done until the saturation curve, for dry and isentropic fluids, or it must be superheated for wet fluids. The transferred heat to the working fluid is

$$\dot{Q}_{eva} = \dot{m}(h_2 - h_3) \quad (4.2)$$

Stage 3 to 4:

The saturated or superheated liquid is expanded in the turbine. In the turbine thermal energy is converted into mechanical energy, which is then later converted to electrical energy.

$$\dot{W}_{t,net} = \eta_t \dot{m}(h_3 - h_4) \quad (4.3)$$

Stage 4 to 1:

The low-pressure working fluid needs to be cooled and condensed. The cooling fluid in the condenser absorbs the heat supplied.

$$\dot{Q}_{con} = \dot{m}(h_3 - h_4) \quad (4.4)$$

And the mass flow of the cooling air is calculated with

$$\dot{m}_{air} = \frac{\dot{m}_{ORC}(h_4 - h_1)}{c_{p,air}(T_{con,in} - T_{con,out})} \quad (4.5)$$

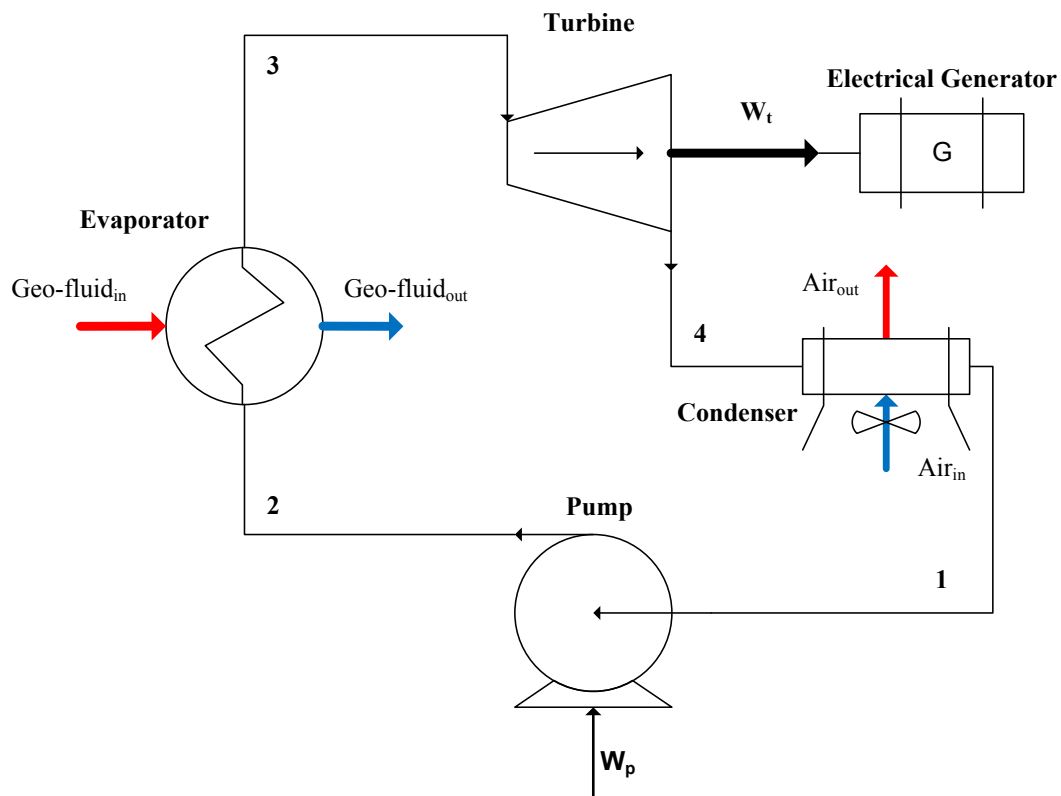


Figure 4.2 Basic components of the ORC

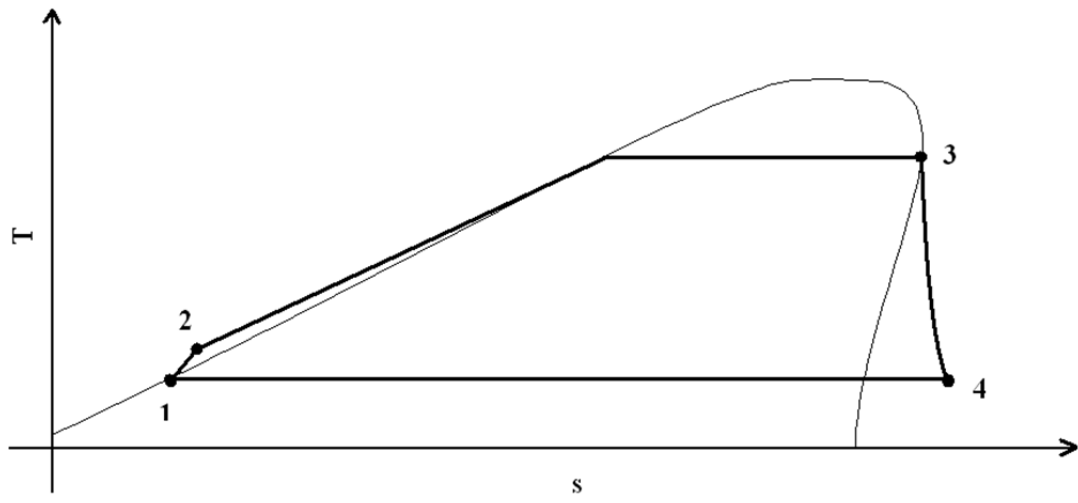


Figure 4.3 T-s chart of the ORC for a dry fluid

4.2 Regenerative Organic Rankine Cycle

The regenerative ORC (RORC) is a variant of the basic ORC. According to Mago (2006), the RORC will represent a performance improvement compared to the basic ORC. On the other hand, the RORC has the same disadvantages like the ORC, the thermal limitation in the operating range. Additional to that, the RORC is more complex and needs more adjustment during operation.

4.2.1 Working fluid

The same criteria for choosing working fluid as were used for the basic ORC apply for the RORC as well, and thus the same working fluid R245fa will be examined.

4.2.2 Design of the RORC

Stage 1-2 and 8-9:

As in the ORC cycle, the pumps create the necessary pressure in the RORC. The pressure of the saturated liquid from the condenser is increased in the low-pressure pump to the one of open-feed-organic-heater (OFOH). Saturated liquid from the OFOH is further pressurized in the high-pressure pump. The required work for the high-pressure pump is

$$\dot{W}_{pHP,net} = \eta_p \dot{m}_{RORC} (h_1 - h_2) \quad (4.6)$$

And for the low pressure pump

$$\dot{W}_{pLP,net} = \eta_p \dot{m}_{RORC} (1 - X_1) (h_8 - h_9) \quad (4.7)$$

Stage 2-3:

The organic liquid leaving the high-pressure pump is sub-cooled. In the evaporator it is heated and evaporated. The transferred heat in the evaporator to the working fluid is

$$\dot{Q}_{eva} = \dot{m}_{RORC} (h_2 - h_3) \quad (4.8)$$

Stage 3-4 and 6-7:

The saturated vapour is expanded in the high-pressure turbine. After the HP-turbine the stream is split and fraction of the flow is further expanded in the low-pressure turbine while the other feeds the OFOH. More details about the OFOH further down. Thermal energy is converted in the turbines to mechanical energy, which is then later converted to electrical energy in the generator. The work for the high-pressure turbine is

$$\dot{W}_{tHP,net} = \eta_t \dot{m}_{RORC} (h_3 - h_4) \quad (4.9)$$

And for the low-pressure turbine

$$\dot{W}_{tLP,net} = \eta_t \dot{m}_{RORC} (1 - X_1) (h_6 - h_7) \quad (4.10)$$

Stage 4-5:

A mass and energy balance determines the fraction of the flow rate that enters the OFOH. For better understandings, see Figure 4.5. The fraction that enters the OFOH can be calculated as

$$X_1 = \frac{h_1 - h_9}{h_5 - h_9} \quad (4.11)$$

The fraction of the flow that enters the low-pressure turbine is determined using equation 3.11.

$$X_2 = (1 - X_1) \quad (4.12)$$

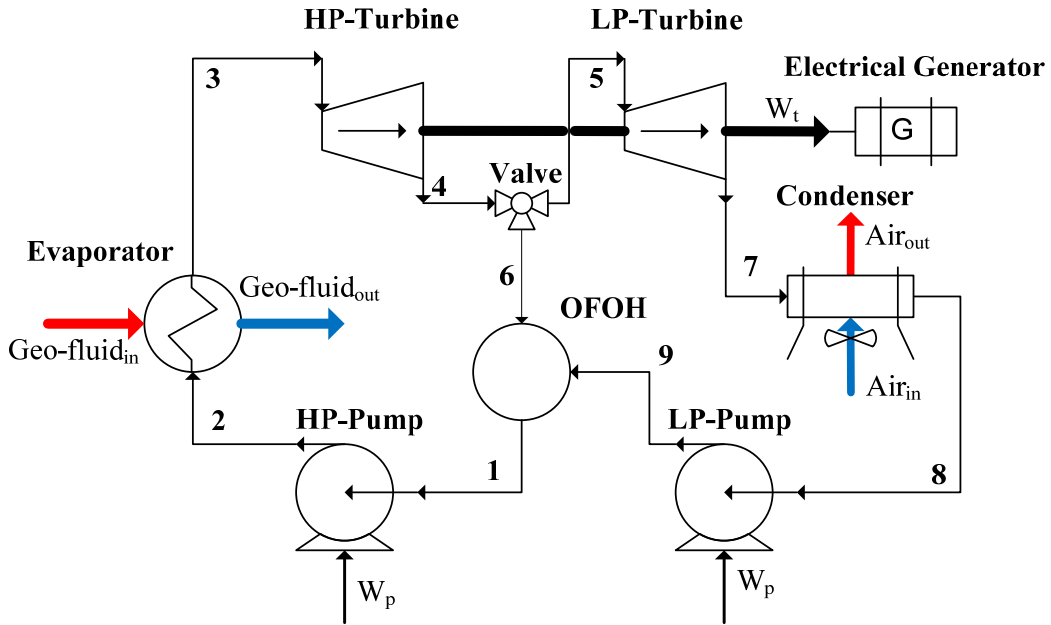
Stage 7-8:

The low-pressure working fluid, which is still superheated, needs to be cooled and condensed to saturated liquid. The cooling fluid in the condenser absorbs the heat supplied.

$$\dot{Q}_{con} = \dot{m}_{RORC}(1 - X_1)(h_3 - h_4) \quad (4.13)$$

The mass flow of the cooling air is calculated with

$$\dot{m}_{Air} = \frac{\dot{m}_{RORC}(1 - X_1)(h_7 - h_8)}{c_{p,air}(T_{con,in} - T_{con,out})} \quad (4.14)$$



4.4 Basic components of the RORC

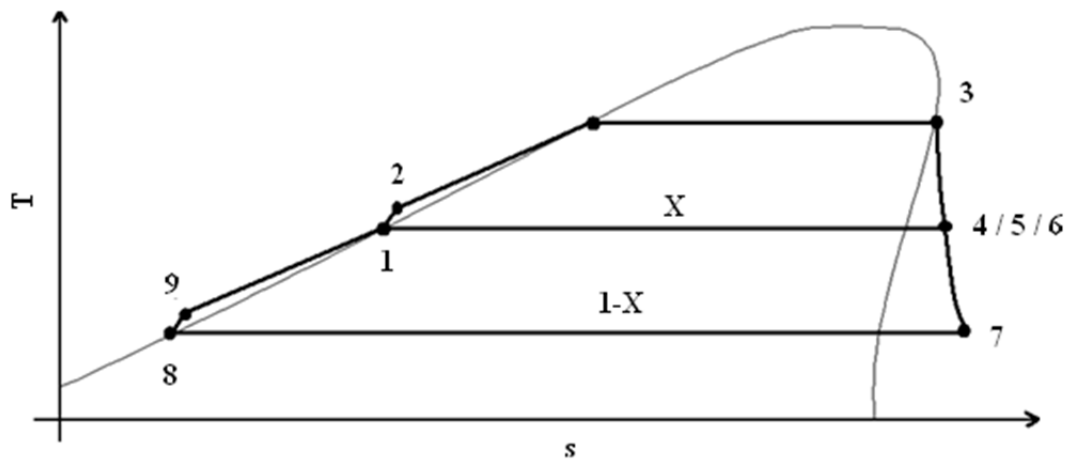


Figure 4.5 Thermodynamic RORC of R245fa

4.3 Stirling engine

The first regenerative cycle invented was the Stirling engine. Robert Stirling patented it in 1816 (Kongtragool, 2006). Kongtragool describes further, that any heat energy source, can be utilized with a Stirling engine. Another advantage of the Stirling engine is that all compressible fluids, even vapour can be used as working fluid. The Stirling engine has many good features such as:

- Multiple fuel usage
- Low engine speed
- Constant power output

There are also some important requirements needed (Zumerchik, 2001):

- Excellent cooling source
- Long warm up time

Today, three different Stirling engine configurations are in use. They can be divided in:

1. Alpha configuration
2. Beta configuration
3. Gamma configuration

All three configurations are shown in Figure 4.6.

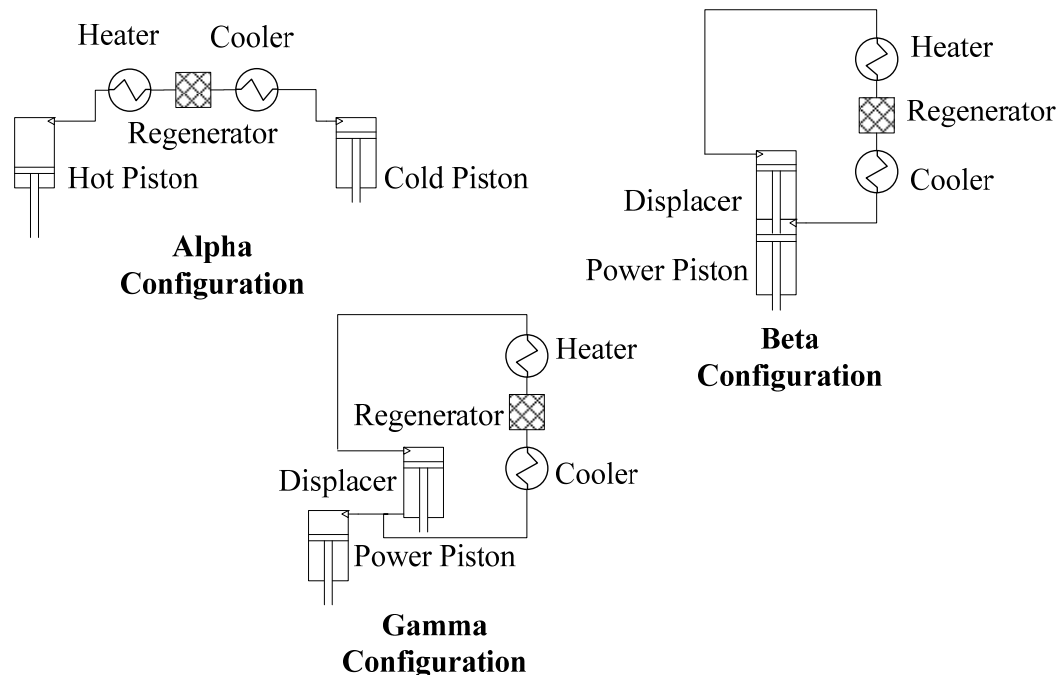


Figure 4.6 Types of Stirling engines configurations

In thermodynamic aspects, they work in the same way, like the one shown in Figure 4.8. But as seen in Figure 4.6, the layout of the piston and displacer differs, while the set up of the heater, regenerator and the cooler is the same. The highest mechanical efficiency is reached with the gamma configuration. (Kongtragool, 2006) When designing the gamma configuration, the vertical type is preferred, to reduce the bushing friction. (Walpita, 1983) The gamma configuration is a low temperature

differential (LTD) Stirling, since it can start working from temperature difference > 0.5 K. Characteristics of the LTD Stirling are:

- Volume ratio between the power piston and the displacer is large
- Large displacer diameter

The LTD Stirling works only to a maximum temperature of 150°C . (Chen, 2003)

4.3.1 Design of the LTD Stirling engine in the gamma configuration

The ideal Stirling-process consists of an isothermal compression/expansion and of isochoric heating/cooling. The process is shown in Figure 4.8. The gamma configuration of the Stirling engine is seen in Figure 4.7. In the Figure, the ideal functional principle is shown. In detail, the different thermodynamic states can be described as follows:

Stage 1-2:

The displacer isothermally compresses the working fluid, while the cooler removes the heat from the working fluid during compression.

Stage 2-3:

The working fluid is heated isochoric in the displacer by the heater.

Stage 3-4:

The working fluid is isothermally expanded in the power piston while the heater continues to heat the gas.

Stage 4-1:

The power piston pushes the working fluid back to the displacer under isochoric conditions while it passes the cooler and gets cooled.

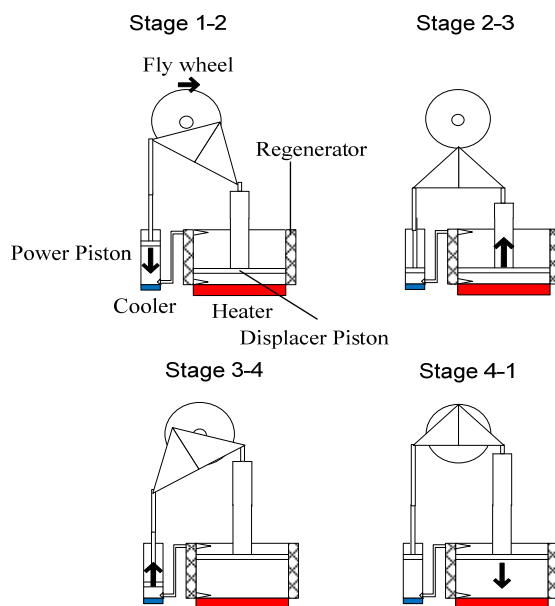


Figure 4.7 Ideal functional principle of the gamma type Stirling engine

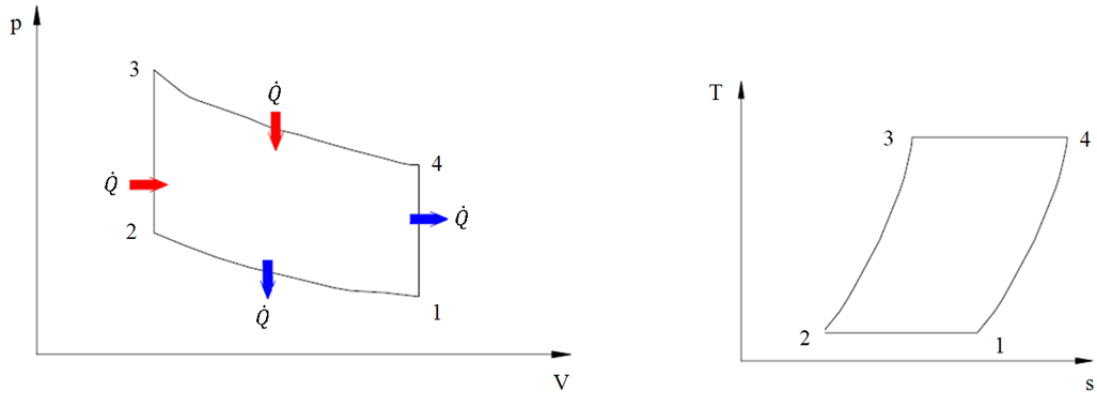
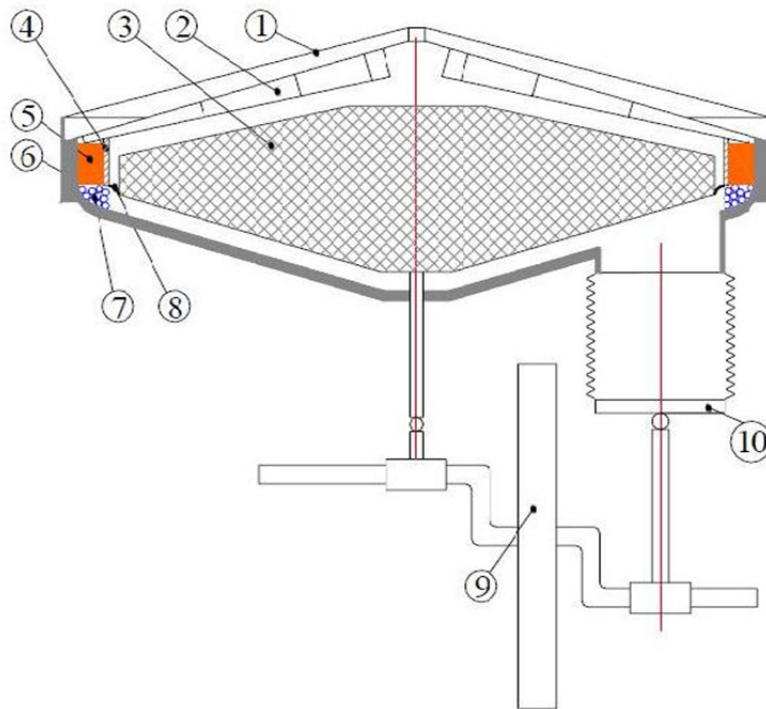


Figure 4.8 p-V and T-s chart of the ideal Stirling process with thermodynamic states

4.3.2 Modelling the LTD Stirling engine

The simulation of the Stirling engine in this study is based on the dissertation of Chen (2003). Chen developed a solar low temperature gamma – type Stirling engine, see Figure 4.9.



- | | |
|--------------------|----------------|
| 1 Cover sheeting | 6 Box |
| 2 Absorber | 7 Cooler |
| 3 Displacer | 8 Membrane |
| 4 Displacer piston | 9 Flywheel |
| 5 Regenerator | 10 Powerpiston |

Figure 4.9 Construction of the solar LTD Stirling (Chen, 2003)

The sizing data for the LTD Stirling engine is shown in Table 4.2. The volumes are explained briefly further down. These data were taken to evaluate the Stirling engine in this study. They rely on the experimental Stirling engine from Chen.

Table 4.2 Sizing data for the LTD Stirling engine

Volumes			Death volumes			Other		
V	168.7	dm ³	V_{TH}	7.7	dm ³	p_m	101.3	kPa
V_{Ar}	9.2	dm ³	V_{TK}	7.7	dm ³	n	35	1/min
V_{VBew}	107.4	dm ³	V_{TA}	18.7	dm ³	m	0.1971	kg
			V_R	27.3	dm ³	ε	1.055	-

Schmidt formula

Gustav Schmidt developed in 1871 a formula to calculate and size a Stirling engine. The Schmidt formula is an isothermal calculation method. There are various forms of the formula to calculate different medium and high temperature Stirling engines, which were approved by experimental studies. According to Chen, there were no publications for low temperature Stirling engines until 2003. In his dissertation, he developed a modified version of the Schmidt formula to evaluate LTD Stirling engines in the gamma configuration. This formula is taken to evaluate the Stirling engine in this Thesis.

The volume of the hot space, V_H , which differ with the time, is calculated with:

$$V_H = V_{VBew}[1 + \cos(\varphi + \alpha)]/2 \quad (4.13)$$

Where V_{VBew} is the maximum variable volume of the displacer, α is the phase angle and φ is the rotation angle.

The cold space volume, that differs with the time as well, is determined with

$$V_K = V_{VBew}[1 - \cos(\varphi + \alpha)]/2 \quad (4.14)$$

And the working volume with

$$V_{Ar} = V_{ArBew}[1 + \cos(\varphi)]/2 \quad (4.15)$$

While V_{ArBew} is the maximum variable working volume.

The constant gas mass, m , is calculated as the sum of the gas masses in the LTD Stirling engine according to:

$$m = \sum_i m_i = m_H + m_K + m_{Ar} + m_R + m_{TH} + m_{TK} + m_{TA} \quad (4.16)$$

With the gas mass m , the temperatures of the hot side T_H , the cold side T_K and the regenerator temperature T_R , the volumes and the death volumes of the hot side V_{TH} , the cold side V_{TK} and of the working space V_{TA} and assuming the ideal gas law, the pressure will be

$$p = \frac{mR}{\frac{V_H}{T_H} + \frac{V_K}{T_K} + \frac{V_{Ar}}{T_R} + \frac{V_R}{T_R} + \frac{V_{TH}}{T_H} + \frac{V_{TK}}{T_K} + \frac{V_{TA}}{T_K}} \quad (4.17)$$

$$\text{With } T_R = \frac{1}{2}(T_H + T_K)$$

Equations 4.13 – 4.15 put in to 4.17 results in

$$p = \frac{mR}{k + \left(\frac{V_{VBew}}{2T_H} \cos\alpha - \frac{V_{VBew}}{2T_K} \cos\alpha + \frac{V_{ArBew}}{2T_K} \right) \cos\varphi + \left(\frac{V_{VBew}}{2T_K} - \frac{V_{VBew}}{2T_H} \right) \sin\alpha \sin\varphi}$$

$$\text{With } k = \frac{V_{VBew}}{2T_H} + \frac{V_{VBew}}{2T_K} + \frac{V_{ArBew}}{2T_K} + \frac{2V_R}{T_H+T_K} + \frac{V_{TH}}{T_H} + \frac{V_{TK}}{T_K} + \frac{V_{TAr}}{T_K}$$

It is defined that,

$$A \sin\beta = \frac{V_{VBew}}{2} \left(\frac{1}{T_K} - \frac{1}{T_H} \right) \sin\alpha \quad (4.18)$$

$$A \cos\beta = \frac{V_{ArBew}}{2T_K} - \frac{V_{VBew}}{2} \left(\frac{1}{T_K} - \frac{1}{T_H} \right) \cos\alpha \quad (4.19)$$

With the area A and the volume expansion coefficient β .

The area A is determined then with

$$A = \frac{1}{2} \sqrt{\left[\left(\frac{V_{ArBew}}{T_K} \right)^2 + \left(\frac{V_{VBew}}{T_H} - \frac{V_{VBew}}{T_K} \right)^2 - 2 \frac{V_{ArBew}}{T_K} \left(\frac{V_{VBew}}{T_K} - \frac{V_{VBew}}{T_H} \right) \cos\alpha \right]} \quad (4.20)$$

While the volume expansion coefficient β is calculated with

$$\tan\beta = \frac{\left(\frac{1}{T_K} - \frac{1}{T_H} \right) \sin\alpha}{\frac{V_{ArBew}}{V_{VBew}T_K} - \left(\frac{1}{T_K} - \frac{1}{T_H} \right) \cos\alpha} \quad (4.21)$$

Equations 4.13 – 4.15 and 4.18 – 4.20 put in to 4.17, the pressure follows:

$$p = \frac{mR/k}{1+k_1 \cos(\varphi-\beta)} \quad (4.22)$$

$$\text{With } k_1 = A/k$$

The Work W_H , W_C and W_{Ar} are for the gases on the hot, cold side as well for the power-piston:

$$W_H = \int_0^{2\pi} p dV_H = -\frac{1}{2} V_{VBew} \int_0^{2\pi} p \sin(\varphi + \alpha) d\varphi \quad (4.23)$$

$$W_K = \int_0^{2\pi} p dV_K = \frac{1}{2} V_{VBew} \int_0^{2\pi} p \sin(\varphi + \alpha) d\varphi \quad (4.24)$$

$$W_{Ar} = \int_0^{2\pi} p dV_{Ar} = -\frac{1}{2} V_{ArBew} \int_0^{2\pi} p \sin(\varphi) d\varphi \quad (4.25)$$

$$W_{cycle} = W_H + W_K + W_{Ar} \quad (4.26)$$

$$W_{cycle} = W_{Ar} = V_{ArBew} \frac{\pi m R}{k k_1} \left(\frac{1}{\sqrt{1-k^2}} - 1 \right) \sin\beta \quad (4.27)$$

The Power is calculated with the correction factor f . The correction factor was introduced by Chen (2003), to adjust the calculated results with his experimental results. The calculated power is then

$$P = f W_{cycle} n / 60 \quad (4.28)$$

$$\text{With } f = 2/3 \quad (4.29)$$

And last but not least, the efficiency is:

$$\eta_{Sch} = \left[\frac{f W_{cycle}}{W_H} \right] * 100 \quad (4.30)$$

5 Simulation

The objective of this part of the Master's Thesis is to identify and compare different technologies to produce electricity from a low temperature heat source, with respect to their efficiency and sustainability. Since pressures in geothermal wells go up to 100 bar and above temperatures from 200°C, the well pressure in this research has been set to 30 bar (Jaya, 2010). Furthermore this pressure was chosen to avoid a two phase of the brine during the evaporation process of the working fluid. Based on a base case with the conditions shown in Table 5.1, each technology is investigated.

Table 5.1 Base case conditions

Base Case	Inlet temperature, T_{in} [°C]	Outlet temperature, T_{out} [°C]
Heat source	160	90
Heat sink	10	20

After investigating the optimum properties in the base case, a sensitivity analysis is done with respect to the heat source and sink. Thereby, the systems' thermal efficiency is calculated, according to the first law of thermodynamics. The system efficiency is evaluated by excel with the following equation 5.1.

$$\eta_I = \left[\frac{W_t - W_p}{\dot{Q}_{eva}} \right] * 100\% \quad (5.1)$$

According to the second law of thermodynamics, the highest reachable thermal efficiency of heat engines is calculated with the Carnot efficiency

$$\eta_C = \left[1 - \frac{T_{min}}{T_{max}} \right] * 100\% \quad (5.2)$$

The Carnot-Factor (CF) is calculated as

$$\eta_{CF} = \left[\frac{\eta_I}{\eta_C} \right] * 100\% \quad (5.3)$$

5.1.1 Assumptions common to all technologies

- The efficiency of the turbine and the pump is set to 0.85
- Pressure drop in the evaporator, condenser and the pipes are neglected
- The work for the cooling- and geothermal-water-pump are neglected
- The minimum temperature approach in the evaporator and the condenser is set to 10 °C
- The geo fluid is assumed to be water
- The minimum reinjection temperature of the geo fluid is set to 90°C to avoid crystallisation of silica in the geo fluid
- The pressure of the geo fluid is set to 30 bar
- The electrical output of the generator corresponds to the net output of the system and has the efficiency of 100%.

5.1.2 Investigated cases

The cycles and engines are investigated based on different cases. These cases are:

For the ORC

1. Base case
 - A base case without superheating
2. Superheating
 - The steam in the evaporator is superheated
3. Varying cooling
 - The minimum cooling air temperature is varied
4. Varying heating
 - The maximum evaporator temperature is varied

For the RORC

1. Base case
 - The same heat source and sink temperature as the one used for the ORC
2. Varying medium pressure
 - The medium pressure between the high, low pressure turbine and in the OFOH is investigated
3. Varying cooling
 - The minimum cooling air temperature is varied
4. Varying heating
 - a. The maximum evaporator temperature is varied

Since the RORC is just a variation of the ORC, the superheating case will be not evaluated again. Instead another case will be performed, to find the optimum pressure ratio between the high, low-pressure turbine and in the OFOH. In the RORC, only the working fluid that had the highest efficiency in the ORC is tested again.

For the LTD Stirling engine

1. Base case
 - Again using the same heat source and sink temperatures as in the other cycles
2. Varying cooling
 - The minimum cooling air temperature is varied
3. Varying heating
 - The maximum evaporator temperature is varied

5.2 Simulation of the ORC

In Aspen plus different modules are combined to build models like the one for the ORC shown in Figure 4.2. The calculation methods used in the simulation are Peng-Robinson and Steam-NBS. The selection of the calculation method is leaded within Aspen plus. The program calculates temperatures, pressures, enthalpy, entropy, duty, mass flow and the power of the different module.

5.2.1 Case 1: Basic

In this case, the cooling and heating curves of the evaporator and the condenser are plotted. Additionally, the system's first law efficiency is calculated, as well as the Carnot efficiency. The minimum and maximum temperatures of the geo fluid and cooling air are listed in Table 5.2. The efficiencies and the Carnot factor are calculated with equation 5.1, 5.2 and 5.3.

Table 5.2 Heat source and sink

	Temperature, T [°C]; inlet/outlet
Geo fluid	90.0 / 160.0
Cooling Air	10.0 / 20.0

Results

The results of the simulation are shown in Table 5.3. The heating curve in the evaporator shows that the minimum temperature approach of ΔT_{\min} is reached; where the working fluid starts boiling, see Figure 5.1. In the condenser, ΔT_{\min} is reached at the condensation temperature of the working fluid, see Figure 5.2. The slope of the cooling air in the condenser illustrates, that the maximum outgoing temperature of the cooling fluid has to be roughly 10°C lower than the condenser temperature T_1 . Compared with the Carnot efficiency, the cycle has only reached 42% of its maximum thermal efficiency.

Table 5.3 Calculated system efficiencies

Carnot efficiency, η_C [%]	System efficiency, η_I [%]	Carnot-Factor, η_{CF} [%]
34.6	14.6	42.0

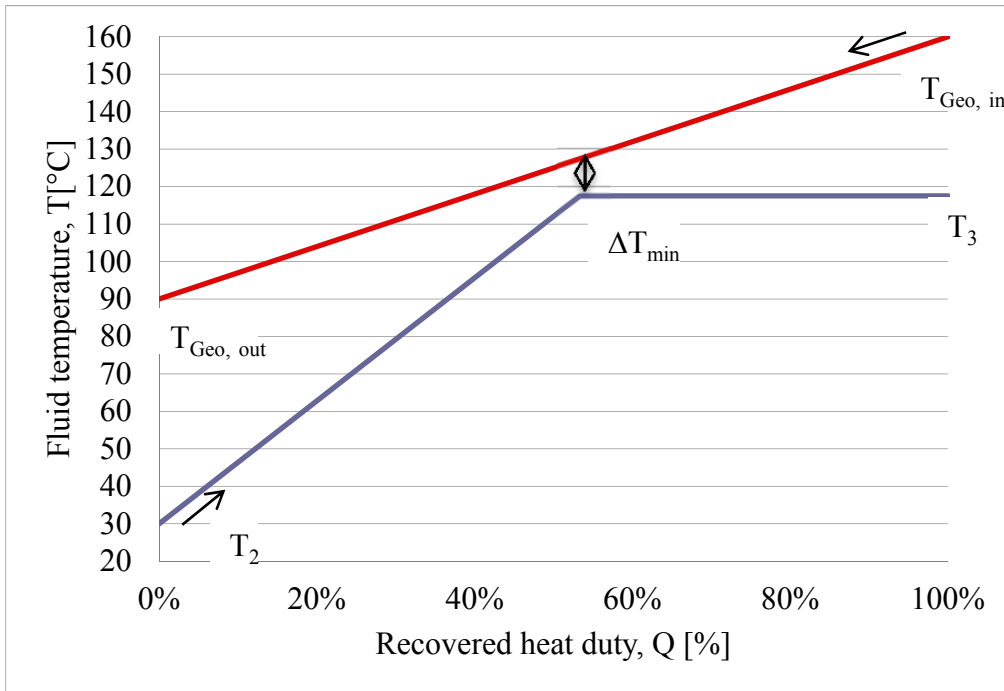


Figure 5.1 Temperature heat transfer diagram for the evaporator

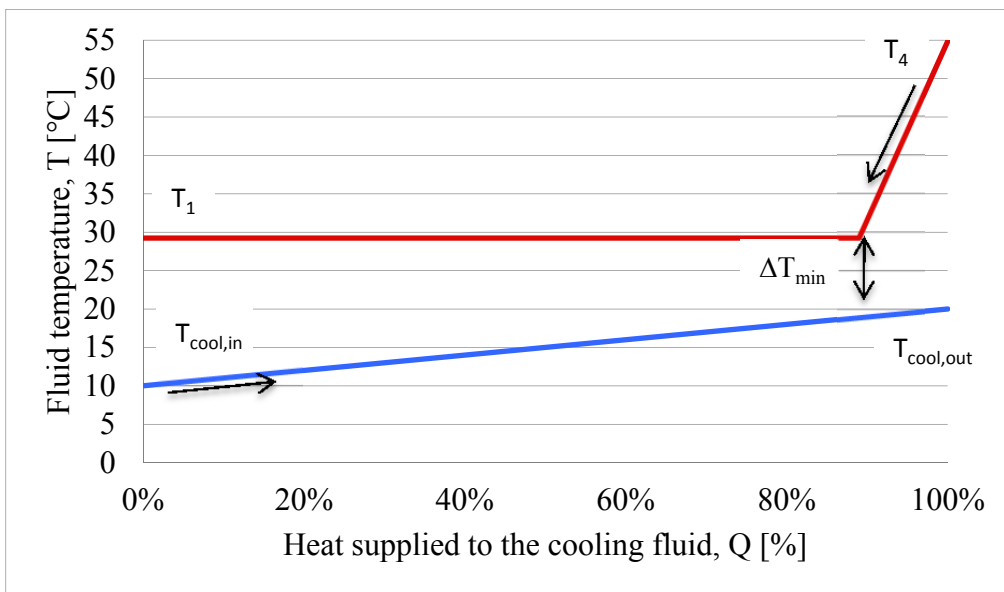


Figure 5.2 Temperature heat transfer diagram for the condenser

5.2.2 Case 2: Superheating

To investigate how superheating influences the cycle efficiency, constant heat and cooling sink is utilized. The assumptions and set values for the case are listed in Table 5.4. The turbine outlet pressure p_4 is kept constant as well as the minimum cycle temperature T_1 .

Table 5.4 Heat source and sink

Temperature, T [°C]; inlet/outlet	
Geo fluid	90.0 / 160.0
Cooling air	10.0 / 20.0

Results

The evaluated results of the simulation are listed in Table 5.5. Superheating showed no efficiency increase; on the contrary, superheating lowered the system efficiency significantly, see Figure 5.4. With an increasing superheating temperature T_3 , the minimum temperature approach between the geo fluid and the working fluid is reached earlier; see Figure 5.5 and Figure 5.6. Consequently the maximum pressure p_2 is lower, compared with no superheating. The higher the working fluid is superheated, the more the pressure has to be lowered and the evaporation starts earlier. That is because of the heating geo fluid slope. See Figure 5.5. The turbine outlet pressure p_4 is kept always constant at 1.7274 bars. While the turbine inlet pressure drops with the increasing superheating temperature. See Figure 5.3. Hence, the higher the pressure ratio p_3/p_4 between turbine in- and outlet, the higher is the efficiency. In Figure 5.5 the geo, which is assumed to be water, and the working fluid, R245fa, are included in the thermodynamic ORC T-s chart. Even so, it is thermodynamically correct and it is added to understand better how superheating reduces the total work (Häßler, 1997).

Table 5.5 Calculated system efficiency at different superheating temperatures

Superheating degree, T [°C]	System efficiency, η_I [%]	Carnot-Factor, η_{CF} [%]
32	13.5	39.0
27	13.6	39.4
22	13.8	39.8
17	13.9	40.3
12	14.1	40.7
7	14.3	41.2
2	14.5	41.8

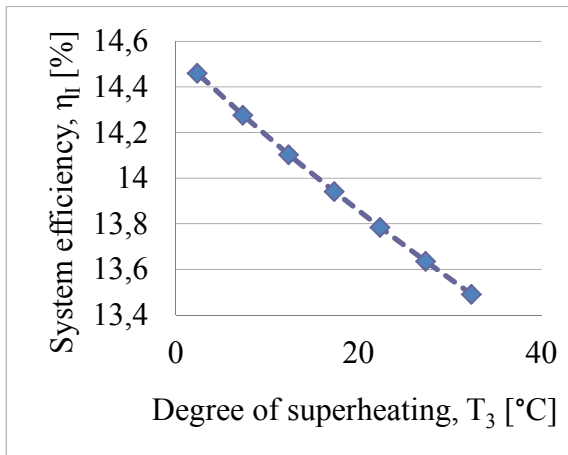


Figure 5.4 System efficiency vs evaporator temperature

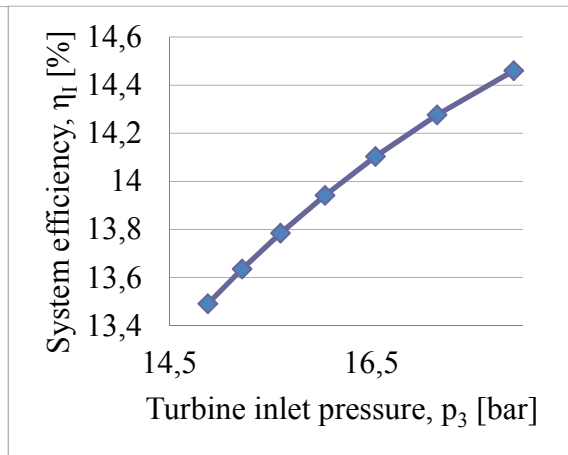


Figure 5.3 System efficiency vs turbine inlet pressure

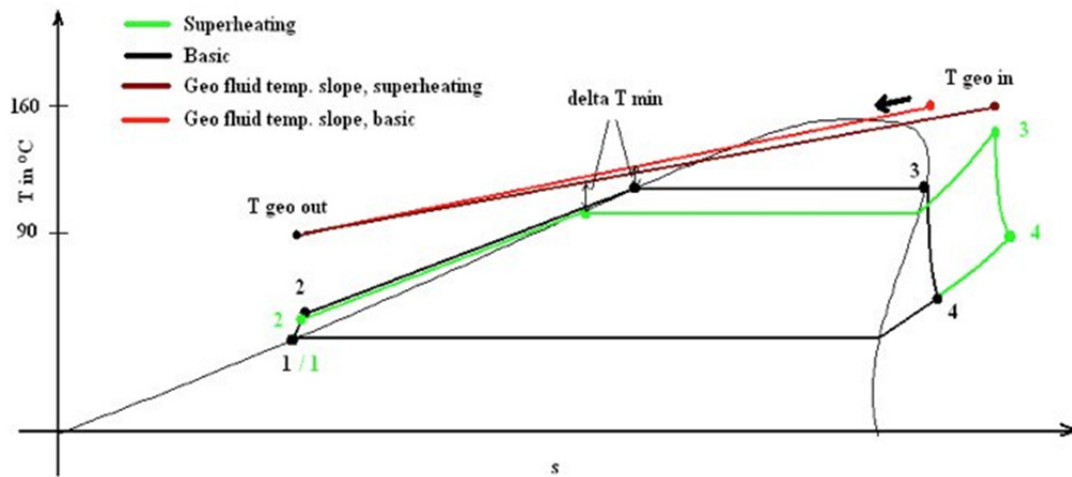


Figure 5.5 Qualitative ORC superheating process in the T-s chart

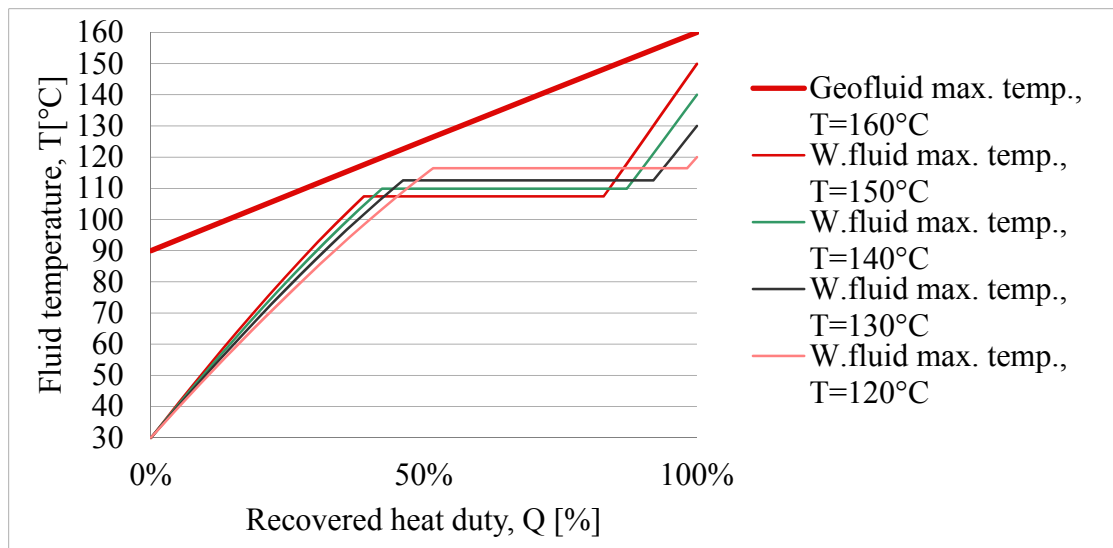


Figure 5.6 Temperature-heat transfer diagram for the evaporator during superheating

5.2.3 Case 3: Varying Cooling

In the previous evaluation, the superheating and the turbine inlet pressure p_3 were investigated. The turbine outlet pressure p_4 influences the system efficiency as well. This is due to the pressure ratio between the turbine in- and outlet. The outlet pressure depends on the minimum cooling temperature. The condensation temperature T_1 , which is roughly 20 degrees hotter than the incoming cooling air, determines the minimum pressure p_4 . A higher cooling air inlet temperature makes it necessary to raise the turbine outlet pressure p_4 . The sensitivity of the ORC's performance on the pressure p_4 is examined under following conditions, see Table 5.6.

Table 5.6 Heat source and sink

	Temperature, T [°C]; inlet/outlet
Geo fluid	90.0 / 160.0
Cooling air	10.0 / 59.0

Results

An increasing cooling air temperature affects the system efficiency significantly; see Table 5.7 and Figure 5.7. As discussed in the previous case, the maximum possible pressure ratio in the cycle affects the efficiency. While superheating does not affect the minimum cycle pressure p_3 after the turbine, a higher cooling air temperature does affect the maximum pressure $p_{2/3}$. With an increasing air temperature the minimum cycle temperature increases as well. This influences the heating of the geo fluid curve and increases the slope of the geo fluid, which in turn decreases the maximum cycle pressure $p_{2/3}$, see Figure 5.9. With increasing air temperature, the system efficiency drops exponential. The ORC stops working with the well and reinjection temperature of the basic case, see Section 5.2.1, at air temperatures over 59 °C. The cooling curves of the condenser are shown in Figure 5.8 for the minimum and maximum inlet cooling air.

Table 5.7 Efficiencies at different condenser temperatures

Condenser temperature, T_1 [°C]	Pressure ratio, p_3/p_4 [bar/bar]	System efficiency, η_I [%]	Carnot-Factor, η_{CF} [%]
29	10.6	14.6	42.0
39	7.0	12.7	39.2
49	4.6	10.6	35.5
59	3.0	8.3	29.9
70	1.8	4.9	19.4
79	1.1	0.5	2.1

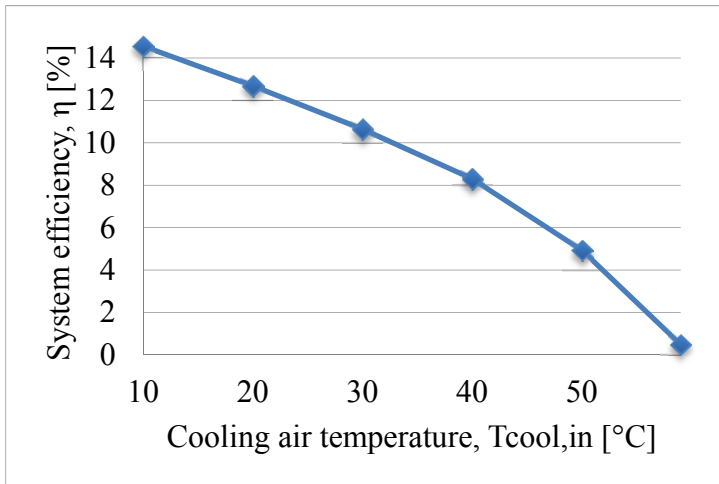


Figure 5.7 System efficiency vs. condenser temperature

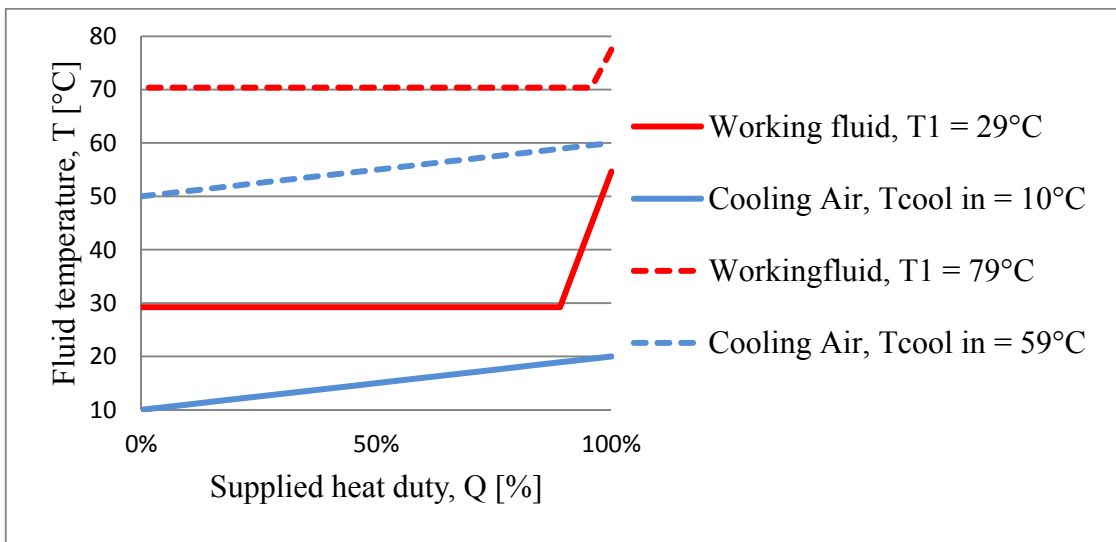


Figure 5.8 Condenser heat curves

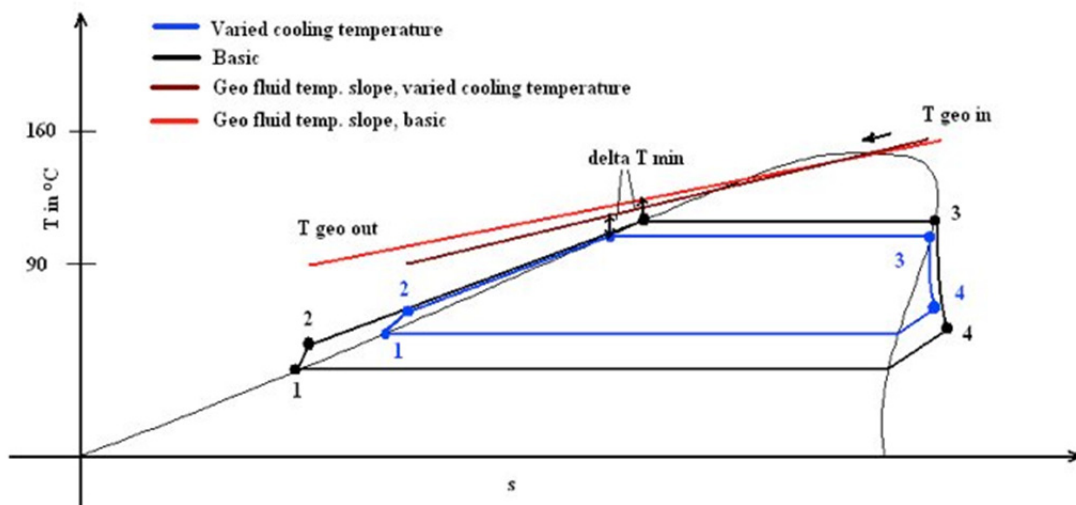


Figure 5.9 Qualitative ORC process in the T-s chart with varied cooling temperatures

5.2.4 Case 4: Varying heating

Considering the previous performance analysis of section 5.2.1 – 5.2.2, the ORC is evaluated from a minimum to a maximum geo fluid inlet temperature of 125°C to 225°C. In this case, the refrigerants introduced in section 4.1.1, R601 and R245fa are tested. Water is tested as well, but with one other condition. Water needs to be superheated; otherwise, droplets emerge during the expansion. The refrigerants were evaluated without superheating. The streams of interest are listed in Table 5.8. The efficiencies are calculated using equation 5.1-5.3.

Table 5.8 Heat source and sink

	Temperature, T [°C]; inlet/outlet
Geo fluid	90.0 / 225.0
Cooling fluid	10.0 / 20.0

Results

The results of the simulation for the different geo fluid inlet temperatures $T_{geo, in}$ are presented in Appendix 1 and plotted in Figure 5.10. Comparing all tested working fluids, R245fa has the best performance with 17.2% system efficiency at a geo fluid temperature of 175°C. N-pentane has a performance of 18.5 % with a geo fluid temperature of 225 °C. When comparing the Carnot-factors, R245fa has up to 43% at a geo fluid inlet temperature of 175°C. While the R601 shows a Carnot-factor at the same temperature of only 32.5% corresponding with a system efficiency of 12%. Water has a way worse efficiency, by far. The system efficiency amounts 10.6% at a geo fluid temperature of 225 °C.

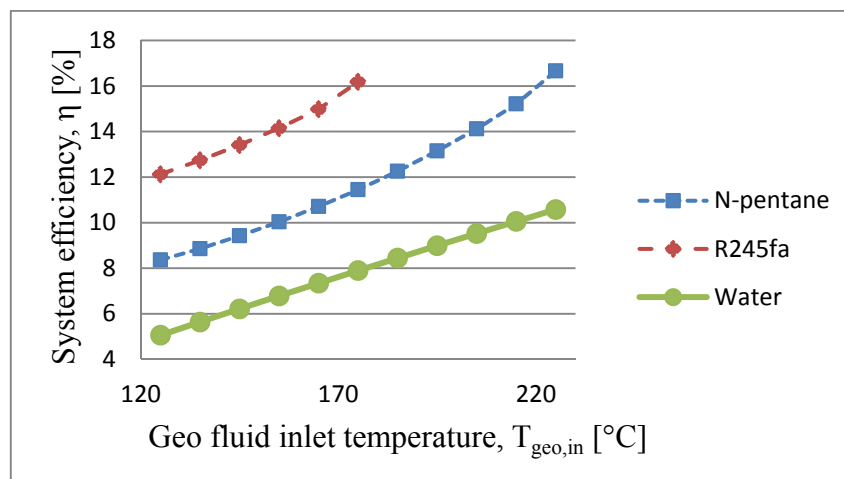


Figure 5.10 System efficiency vs. geo inlet temperature

5.3 Simulation of the RORC

R245fa was identified to be the best working fluid for the ORC in terms of efficiency and sustainability. Therefore, only R245fa will be tested for different heat source temperatures in the RORC.

5.3.1 Case 1: Basic

As in the base case for ORC, the system's first law efficiency is calculated, as well as the Carnot efficiency and factor. The minimum and maximum temperatures of the geo fluid and cooling air are listed in Table 5.9.

Table 5.9 Heat source and sink

	Temperature, T [°C]; inlet/outlet
Geo fluid	90.0 / 160.0
Cooling Air	10.0 / 20.0

Results

The results of the RORC simulation can be seen in Table 5.10. The base case of the RORC, reaches a maximum efficiency of 15.1% corresponding with a Carnot-factor of 43.6%. The maximum pressure in the cycle is 16.3 bar. Compared with the base case of the ORC, see Section 5.2.1, the maximum pressure is in the RORC lower. The reason is the OFOH. The OFOH heats the low pressurized working fluid with the bleed stream X_1 from 29°C to 45°C. As in Section 5.2.3 explained, does the slope of the heating geo fluid in the evaporator set the maximum pressure when the working fluid and the geo fluid reach the minimum temperature approach, see Figure 5.9 and Figure 5.11. Summarized, the fewer slopes the heating geo fluid curve has, the higher would be the maximum pressure and temperature. The cooling curves of the condenser are shown in Figure 5.12.

Table 5.10 Simulation results

	Temperature, T [°C]; min/max	Pressure, p [bar]; min/max	η_i [%]	η_{carnot} [%]	η_{CF} [%]
Working fluid R245fa	30.0 / 112.0	1.7 / 16.3	15.1	34.6	43.6

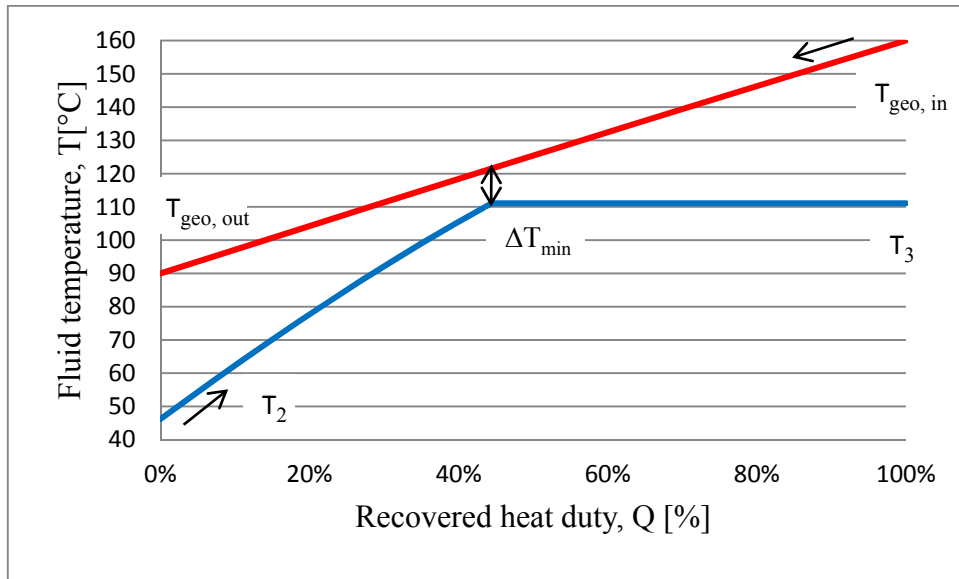


Figure 5.11 Temperature-heat transfer diagram for the evaporator

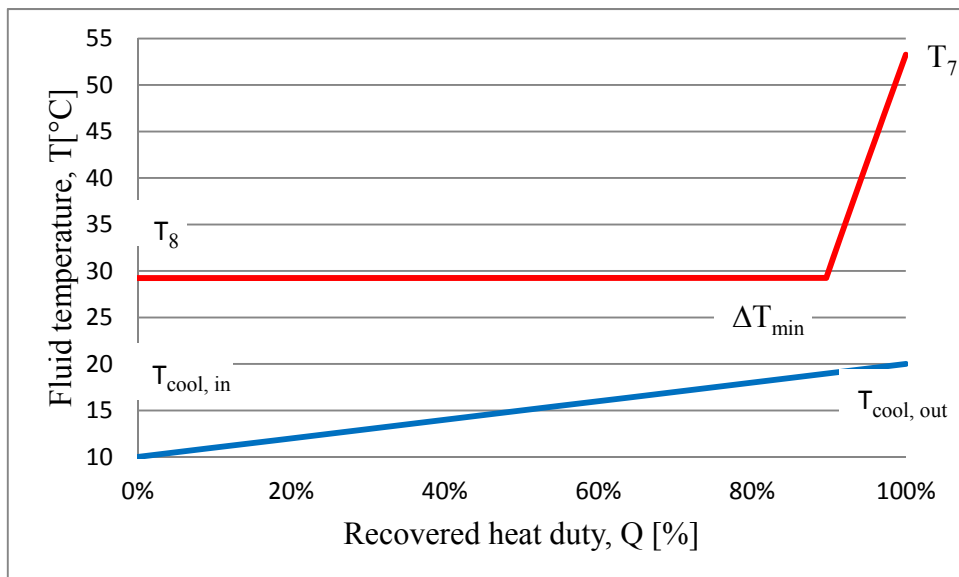


Figure 5.12 Temperature-heat transfer diagram for the condenser

5.3.2 Case 2: Varying feed organic fluid pressure

The mass flow of the feed stream for the OFOH depends on the pressure after the high-pressure turbine. To evaluate the highest efficiency, the OFOH pressure is varied. This was performed using the same heat sink and source utilized as in the base case. In the base case, a pressure of 3 bar was chosen, for the medium pressure.

Results

The results are shown in Figure 5.13. The feed-organic-fluid pressure does not change the system efficiency significantly. Figure 5.13 shows that a pressure change of 0.4 bar, changes the efficiency by approximately 0.045 %. To find the optimum feed-organic-fluid pressure, the OFOH pressure has to be varied in order to find the

optimum pressure, when varying, the cooling air or the heating geo fluid. The chosen medium pressure of 3 bar in the base case was very close to optimum pressure. In fact, the highest efficiency is reached with a pressure around 3.055 bar.

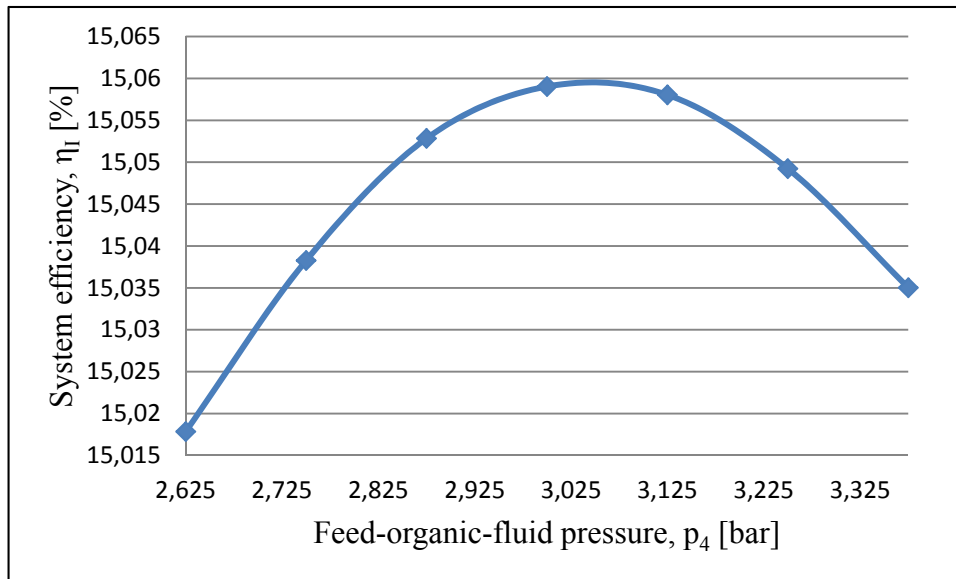


Figure 5.13 Effect of varying feed-organic-fluid pressure on system efficiency

5.3.3 Case 3: Varying cooling

The minimum cooling air temperature is varied in this case. It is the same heat sink utilized with a geo inlet temperature of 160°C and reinjection temperature of 90°C. The medium pressure has to be researched for every temperature increase to determine the highest efficiency.

Results

The system efficiency versus the cooling air temperature is plotted in Figure 5.14. The figure shows that the system efficiency approaches zero for a cooling air temperature of 59°C. At a cooling air temperature of 60°C the cycle is not able to work at the heat source conditions of the base case.

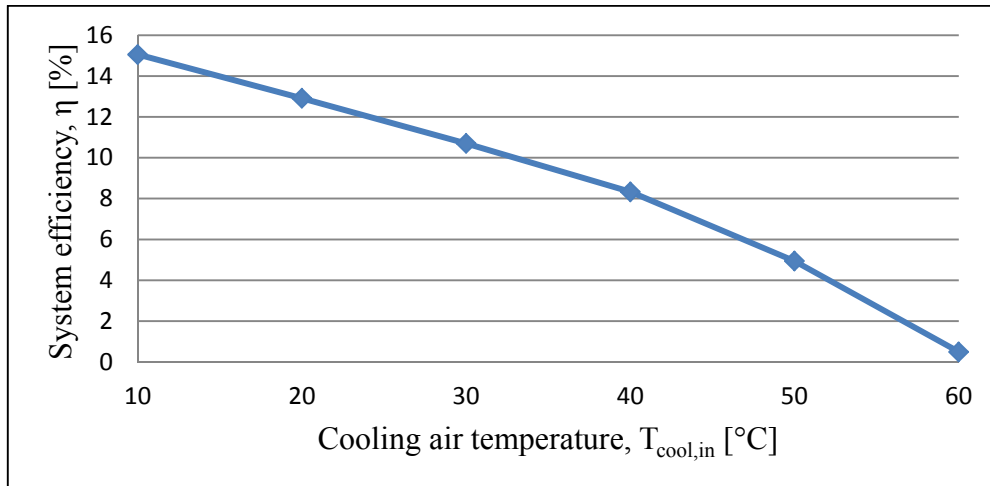


Figure 5.14 System efficiency for different cooling air temperatures

5.3.4 Case 4: Varying heating

The geothermal water inlet temperature is varied while the outgoing temperature is kept constant at 90°C. The same cooling sink as in the base case is utilized with an inlet air temperature of 10°C and an outlet air temperature of 20°C. For each temperature increase a new optimal medium pressure exists.

Results

The results of the simulation are shown in Figure 5.15. The RORC has a maximum temperature operating range from 125°C. up to 185°C with the working fluid R245fa. This limitation is due to the critical pressure of R245fa, which is 36.4 bar. At a geo fluid inlet temperature of 185°C, a pressure of almost 35 bar is reached. The efficiency slope shows an exponential behaviour and the maximum efficiency is 18.5%.

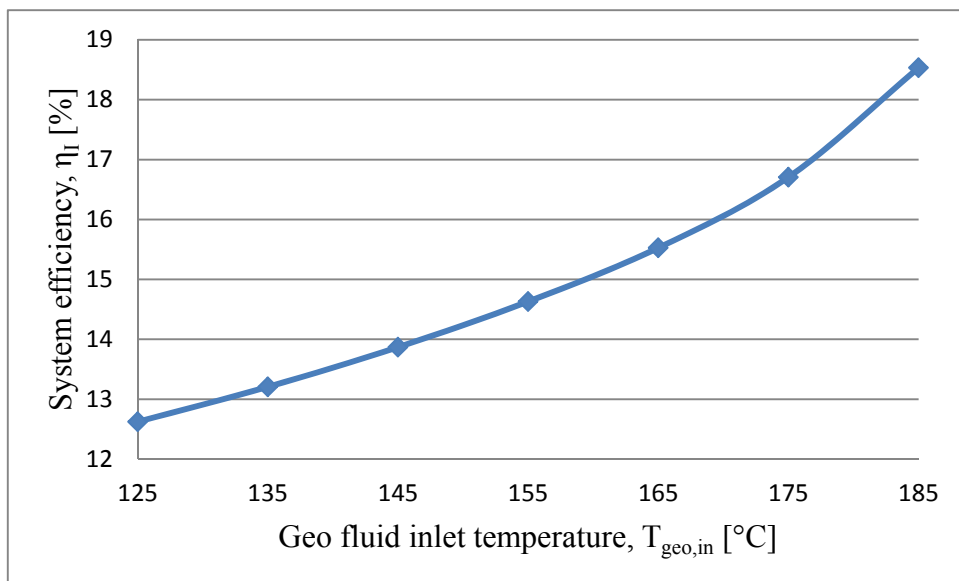


Figure 5.15 System efficiency vs. geo inlet temperatures

5.4 Simulation LTD Stirling engine

5.4.1 Case 1: Basic

The LTD Stirling engine in the gamma configuration has a maximum working temperature of 150°C. The base case has a geo inlet temperature of 160°C. The minimum temperature difference is as previously set to 10°C. The temperature and the pressure ratio ϵ (i.e. the maximum compression ratio within) inside the Stirling engine can be seen in Table 5.11.

Table 5.11 Heat source and sink

	Temperature, T [°C]; min/max	Pressure ratio, ϵ
Geo fluid	90.0 / 160.0	-
Cooling Air	10.0 / 20.0	-
Working fluid, Air	20.0 / 150.0	1.055

Results

The LTD Stirling engine shows a very high efficiency for the base case. The efficiency is calculated with the Schmidt theory according to equation 4.30. The system efficiency has a value of 18.3%, which represents a Carnot-factor of 52.8 %, see Table 5.12.

Table 5.12 System efficiency's for the LTD Stirling engine

System efficiency, η_{Sch} [%]	Carnot efficiency, η_c [%]	Carnot-Factor, η_{CF} [%]
18.3	34.6	52.8

5.4.2 Case 2: Varying cooling

Previous cases where the cooling was varied showed that the cycles were very sensitive to the cooling temperature. In order to analyse the LTD Stirling engine, the cooling air temperature is increased in steps of ten degrees starting from the base case with a cooling air temperature of 10°C and ends at a temperature of 60°C.

Results

In Figure 5.16 the results of the calculation are shown. The LTD Stirling engine efficiency slope shows a linear behaviour for the varied cooling air temperatures, starting at an efficiency of 18.3% and ending at an efficiency of 11.2%. The efficiency decreases almost 1.4% every 10 degrees.

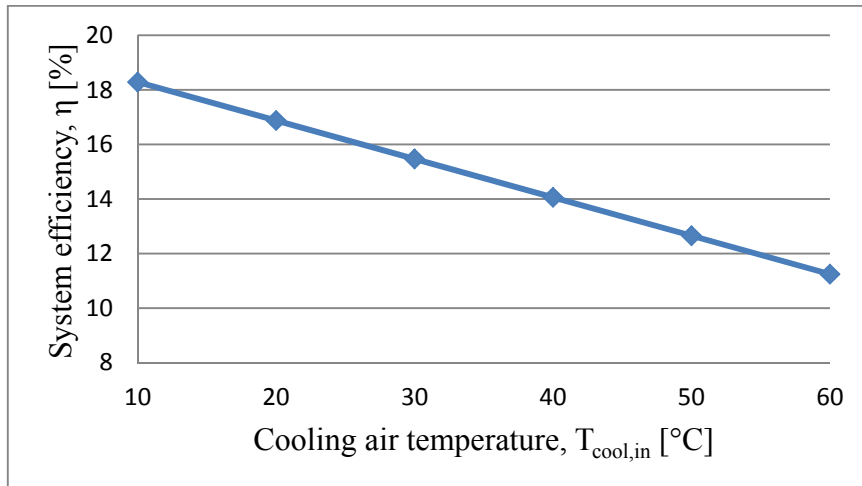


Figure 5.16 System efficiency for different cooling air temperatures

5.4.3 Case 3: Varying heating

As for the previous cycles, the geo fluid inlet temperature is varied from 125°C to a maximum temperature of 160°C.

Results

Figure 5.17 shows the calculated efficiency for different geo inlet temperatures. The heating efficiency curve shows a linear increasing efficiency. The efficiency increases almost 1.1% every ten degrees, from 14.6% to 17.8% efficiency.

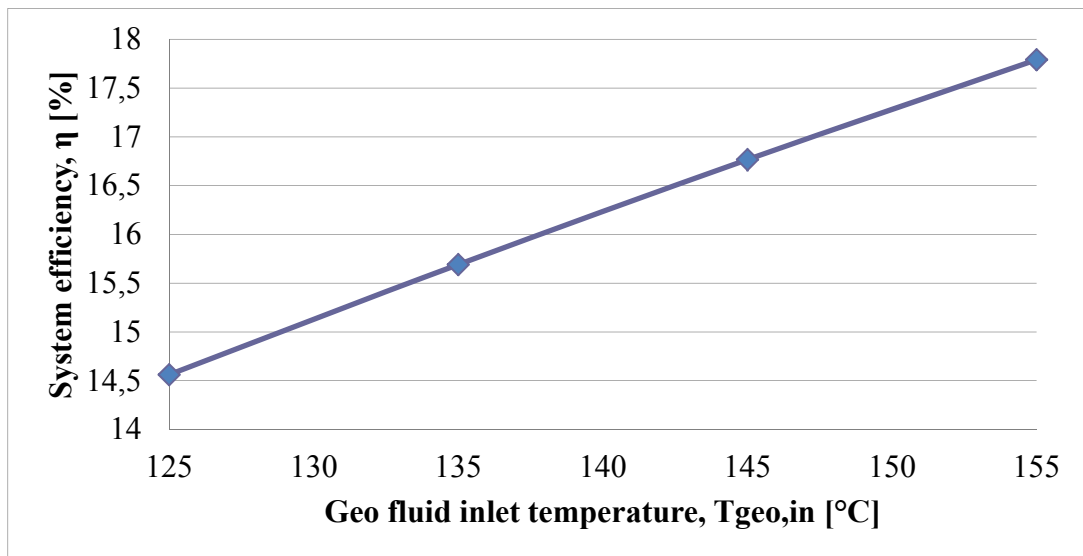


Figure 5.17 System efficiency vs. geo inlet temperatures

6 Economics

At first some words on the location and local climate data since the power cycles are air-cooled and the air temperature plays a key role in the performance. The location of the climate data is from Munich and was chosen without any reason. The analysis is split in two parts. At first, the cycles are simulated during the summer and then during the winter. The two different cases, in which the power cycles are evaluated, are:

- Summer case
 - The average temperature in the summer is evaluated. For simplicity reasons, the summer months are from the beginning of April until the end of September.
- Winter case
 - The average temperature in the winter is evaluated from the beginning of October until the end of March.

The climate data are based on the data from the webpage eklima.de. During the simulations and evaluations, an average temperature of 15°C for the summer and 2°C for the winter were chosen, for simplicity reasons. The detailed average evaluation is in the Appendix 3.

The availability of the plant is assumed to be 95%. This gives an average operating hours per year for the cycles of 8322 hours. The heating fluid in the evaporator has a mass flow of 550 t/h (personal communication with G. de Caprona, Geotermica). Based on that, the average power output for the whole year is calculated and multiplied with different feed in tariffs for each cycle up to 0.3 €/kWh. According to the European Commission, electricity generated from renewable sources and is produced by companies or individuals are bought by EU member states. The prices paid for those “self-produced” electricity is called “feed in tariff” (European Commission, 2011).

Results

In Figure 6.1 – 6.3 the profit for an ORC, RORC and LTD Stirling plant is shown dependent on the electricity price. The LTD Stirling plant is the most profitable for temperatures of up to 155°C. Above these temperatures, the RORC plant is the most economical.

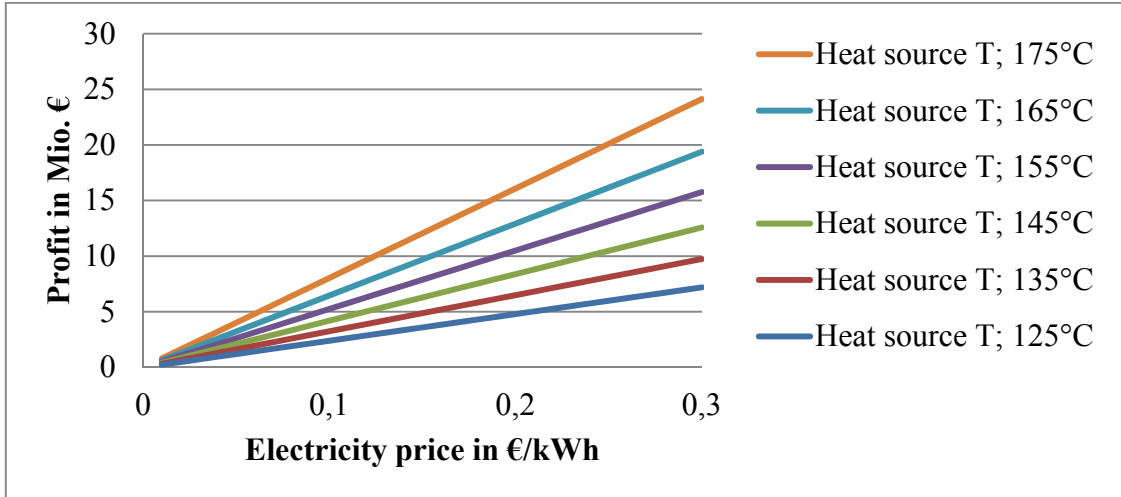


Figure 6.1 Profit of the ORC plant dependent on the electricity price

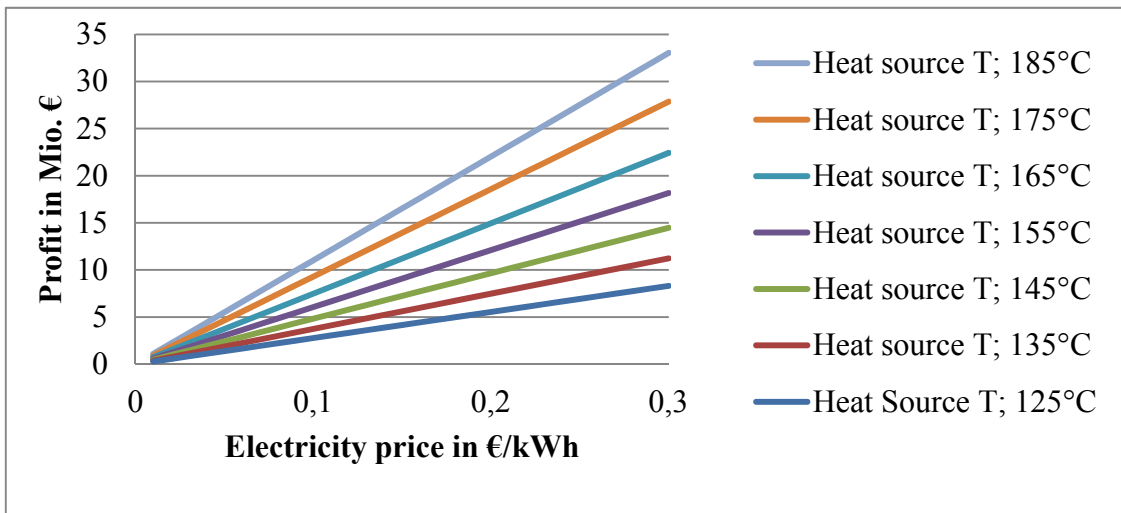


Figure 6.2 Profit of the RORC plant dependent on the electricity price

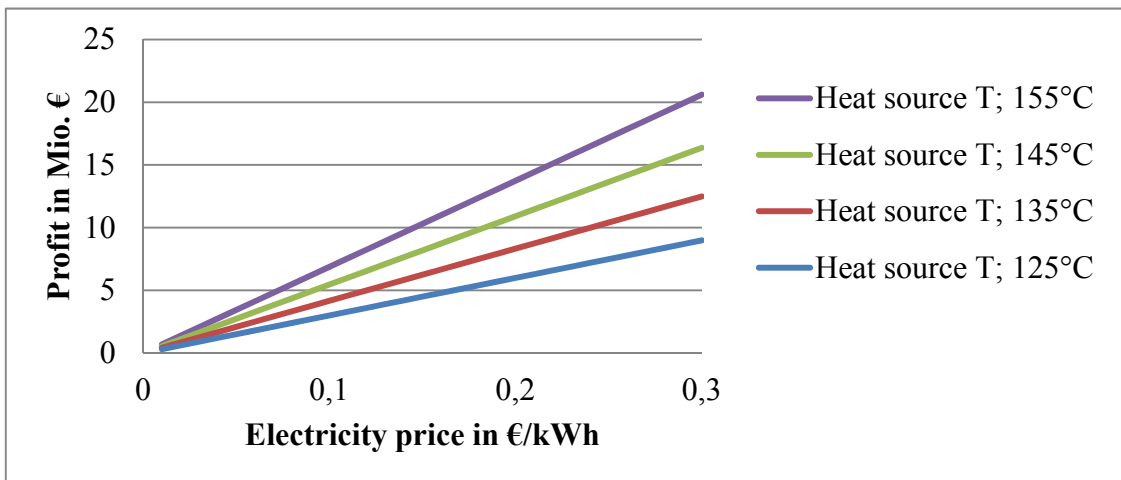


Figure 6.3 Profit of the LTD Stirling plant dependent on the electricity price

7 Geotermica

Geotermica was founded in 2009. The major shareholder of the company is Guy C de Caprona, as well the contracting authority for this Thesis. Geotermica is a company, which is exploring medium geothermal temperature sources within a temperature range from 100°C to 200°C (Geotermica AB). Geotermica is interested in looking at different alternatives for low temperature electricity production cycles. This was done earlier in this Thesis. Only the ORC and RORC, which can be realized in near future for electricity production, will be evaluated for the Geotermica case. Due to missing economic information's about the LTD Stirling engine. Based on those results and together with the expected well flows at the Aeolian Islands in the south of Italy, which Geotermica will explore, the low temperature electricity production cycles are evaluated. In the first part of this chapter, the power cycles are further investigated. According to the weather data gathered from the data base of eklima.de and the expected well flows of the Aeolian Islands, the efficiency of the cycles of interest are evaluated. Further on, in the second part of this chapter, an economic analysis is performed.

7.1 Technical analysis

The expected well flows of the Aeolian Islands and the weather data are shown in Table 7.1. Based on these values, the efficiency for the ORC and the RORC are calculated. The average temperature in the summer is 23°C and during wintertime 15°C. When comparing the two power cycles, the RORC shows a slightly higher performance, see Table 7.2. and Table 7.3. If the RORC is still the best choice from the economical point of view will be analysed in the next chapter.

Table 7.1 Aeolian Islands well data and weather data (Geotermica AB and eklima.de)

Well data		Weather data		
Unit	Temperature	Flow rate	Average temperature	
			Summer	Winter
	°C	t/h	°C	°C
	150	550	22.5	14.6

Table 7.2 Efficiency's for the ORC and RORC for the Geotermica case in the summer

Summer	ORC	RORC
	Unit	
System efficiency, η_I	%	12.7
Carnot efficiency, η_{carnot}	%	30
Carnot-Factor, η_{CF}	%	42.3

Table 7.3 Efficiency's for the ORC and RORC for the Geotermica case in the winter

Winter		ORC	RORC
		Unit	
System efficiency, η_I	%	14.1	15
Carnot efficiency, η_{carnot}	%	31.9	31.9
Carnot-Factor, η_{CF}	%	44.2	46.7

7.2 Economic analysis

As shown in Table 7.1, the cycles are evaluated in two cases. The size of the equipment is based on the simulation for both cases. During wintertime, the highest power demands for the pumps and turbines are needed / produced as well as the largest evaporator area is needed. While during summer time, the highest cooling demand is necessary. Table 7.4 lists which time case is used to design the equipment and to calculate the corresponding investment costs. The price is calculated with an exchange rate of 0.7 \$/€

Table 7.4 Equipment time sizing dependency

Equipment	Turbine	Pump	Evaporator	Condenser	OFOH
Time	Winter	Winter	Winter	Summer	Winter

The purchased equipment cost C_e on a US Gulf Coast basis, January 2007 (CE index (CEPCI) = 509.7, NF refinery inflation index = 2059.1) is evaluated with equation 7.1.

$$C_e = a + bS^n \quad (7.1)$$

Where a and b are cost constants. S is the size parameter and n is the exponent for the type of the equipment. To update the summarized equipment costs to the year 2011, C_e is multiplied with 1.0455. (CECPI10 = 532.9 (Chemical Engineering, 2011) / CEPCI07). To exchange the cost basis to Europe, the equipment costs are multiplied with a location factor for Italy of 1.14. The fixed capital investment is calculated as followed. First of all, the inside battery limits costs C are calculated. Using equation

$$C = \sum_{i=1}^{i=M} C_{e,i,A} [(1 + f_p) + (f_{er} + f_{el} + f_i + f_c + f_s + f_l)/f_m] \quad (7.2)$$

With $C_{e,i,A}$ is the equipment costs in stainless steel. $C_{e,i,A}$ is calculated, using the summarized equipment costs and multiplying it with the material factor f_m which can be found in Appendix 4. f_p is the installation factor for piping and f_{er} is the installation factor for equipment erection. f_{el} , f_i , f_c , f_s and f_l are the installation factors for electrical work, instrumentation and process control, civil engineering work, structures and buildings and last but not least, for lagging, insulation or paint. The detailed factors are tabled in Appendix 4. The total fixed capital cost CFC are estimated with equation 7.3.

$$C_{FC} = C(1+OS)(1+D\&E+X) \quad (7.3)$$

OS are the offsite costs, $D\&E$ are the design and engineering costs and X is the contingency cost. This calculation does not include taxes or inflation. With an interest

rate of 6.5% and an amortisation time of seven years, the annualized capital costs are estimated. (Geotermica) The annualized capital costs of the power plant are calculated with the annual capital charge ratio (ACCR). (Chemical Engineering Design, 2009)

$$ACCR = \frac{[i(1+i)^n]}{[(1+i)^n - 1]} \quad (7.4)$$

Where i is the interest rate and n the number of years. The ACCR is multiplied with the plant costs to get the annualized capital ratio. The feed-in tariff for Italy is 0.2 €/kWh, for plants with a capacity of up to 1 MW (Geotermica). Plants with a capacity over 1MW sells the electricity like any other electricity producer for around 0.07€/kWh and can additionally sell green certificates on the market for around 0.08 €/kWh (Geotermica). The average operating hours for the cycles is expected to be 8322 hours per year (Geotermica). Based on that, the average power output for the whole year is calculated. With the power output, the annual income is evaluated for an electricity price of 0.15€/kWh per year. Last but not least, the payback time in years is estimated for the whole plant including drilling and exploration costs.

$$\text{Payback time} = \text{total costs} / \text{annual income} \quad (7.5)$$

Results

The equipment costs are presented in Table 7.5 for the ORC and RORC in k€. The summarized costs show, that the RORC equipment is roughly 200 k€ more expensive. The major parts of the additional costs are the larger turbine and evaporator. The detailed costs for the whole plant are shown in Table 7.6. The lion's shares of the costs are the exploration and drilling costs with 30 Mio. €. Although the RORC plant is 1.3 Mio € more expensive, it is more economical. This is due to enhanced electricity production of the RORC of 6 GWh per year, see Table 7.7.

Table 7.5 Equipment costs for the ORC and the RORC

Technology	Equipment price in k€					Σ in k€
	Turbine	Pump/-s	Evaporator	OFOH	Condenser/ Air heat exchanger	
ORC	717.2	16.1	279.0	-	235.7	1248.1
RORC	806.9	35.1	336.4	12.1	245.8	1436.4

Table 7.6 Costs estimation and payback time

	ORC		RORC	
Total geothermal Plant costs	8.9	Mio. €	10.2	Mio. €
Exploration and drilling costs	30.0	Mio. €	30.0	Mio. €
	38.9	Mio. €	40.2	Mio. €
Annual Income	5.4	Mio. €	6.3	Mio. €
Payback time	7.2	Years	6.4	Years

Table 7.7 Expected yearly electricity production

Unit	ORC	RORC
GWh	36	42

8 Results and discussion

8.1 Comments on the assumptions

Efficiency

The efficiency of the turbine-/s and pump-/s is set to 0.85. This is typical efficiency used in these types of simulations. With a higher efficiency, the net electricity production would increase and vice-versa.

Pressure drops

Pressure drop in the evaporator, condenser and the pipes are neglected. This results in slightly higher system efficiency in the simulations than in reality. On the other hand, the gain in efficiency is small, thus this assumption is believed to be reasonable.

Geothermal and cooling pump work

The work needed for the cooling- and geothermal-fluid-pump is neglected. This again results in a higher efficiency in the simulations. The cooling pump work, however, is compared with the geothermal-fluid pump very small. Also the work for the geothermal-fluid pump varies with the geological conditions and cannot be exactly predicted until the earth has been explored.

Minimum temperature approach

The minimum temperature approach in the evaporator and the condenser is set to 10 °C. With a smaller temperature approach, the overall system efficiency is increased, but the investment costs for the evaporator and condenser will increase and vice-versa.

Geo fluid

The geo fluid is assumed to be water. Silica and other containments in the geo fluid are varying with each geothermal well. Fouling in the evaporator is not considered in this Master's Thesis.

Reinjection

The minimum reinjection temperature of the geo fluid is set to 90°C to avoid crystallisation of silica in the geo fluid. A higher reinjection temperature would lower the overall energy yield, but would increase the efficiency. On the one hand, a lower reinjection temperature increases the energy yield. But on the other hand, it is necessary to remove silica and other content in the geothermal fluid. This makes the utilization process more complex and expensive.

Pressure

The pressure of the geo fluid is set to 30 bars. The pressure has little effect on the efficiency as long as the fluid remains to be a fluid. With a lower pressure, the geo fluid would pass through various phases in the evaporator as it cools and heats the working fluid. Depending on the pressure, the liquid cools down from superheated

state to a sub cooled state. During this process, the geo fluid has no constant slope. This results in a lower efficiency, since the minimum temperature approach of the working and heating fluid is reached earlier.

Electrical Generator

The electrical output of the generator corresponds to the net output of the system and has the efficiency of 100%. Normally, generators have efficiencies over 90%. Some new generators have an efficiency of 99% (Schwab, 2006). A lower efficiency would lower the electricity production.

8.2 ORC / RORC

The analysis of the ORC pointed out that superheating decrease the system efficiency. Varying the turbine inlet pressure showed, the higher the pressure ratio, the higher is the efficiency. For R245fa two parameters limit the pressure increase, the critical pressure and the evaporator temperature. The performance of the system is very sensitive to the cooling system. While in the base case the system efficiency has a value of 14.6%, the system efficiency had only a value of 10.6% when a minimum cooling air temperature of 30°C was available. The evaluation of the different heat sources from 125°C to 175°C, confirmed the investigation of varying the turbine inlet pressure since the efficiency increased with a higher turbine inlet pressure. Depending on the heat source, the efficiency varies between 12.8% and 17.2% for R245fa, while R601 shows a lower efficiency at these temperatures. However R601 has a higher critical temperature and can therefore handle higher temperatures. It showed a maximum efficiency of 18.5% at a heat source temperature of 225°C. One disadvantage of R245fa is that it has its maximum working temperature in an ORC of 175°C, while R601 can be used for temperatures up to 225°C.

The medium pressure between the high-pressure turbine and the low-pressure turbine in the OFOH was investigated. It showed that a pressure change of 0.5 bars of the optimum OFOH pressure has an efficiency change of approximately 0.04% efficiency. When varying the cooling air temperature, the RORC showed the same behaviour like the ORC. In fact, the RORC has at a cooling air temperature of 30°C or higher, almost the same efficiency like the ORC, see Figure 8.1. In general, the cooling curves of the RORC do not differ so much from the ORC. In Figure 8.2 the heating curves of the ORC and the RORC are shown. The RORC has the same efficiency growth rate as the ORC. But the system efficiency of the RORC is always 0.5% more efficient when varying the heat source temperature. Along with the higher efficiency of the RORC compared with the ORC, the RORC is able to work at a higher heat source temperature with the same working fluid R245fa. This goes hand in hand with a higher maximum efficiency of 18.5%.

The ORC/RORC is today a common technology to produce electricity from low temperature heat sources. Some companies, like GMK or Turboden are specialized on the ORC. The key of the high efficiency of the ORC compared with a normal Rankine cycle is the working fluid. On the one hand, the working fluid increases efficiency, but on the other hand, it also limits the efficiency. The efficiency is limited by the critical pressure of the working fluid. Since the ORC consists of the same components like a “normal” Rankine cycle, the ORC will profit from all new developments.

8.3 LTD Stirling engine

When varying the cooling air temperature, the LTD Stirling engine showed a linear efficiency decrease of approximately 1.4% every ten-degree. Starting with efficiency for the base case of 18.3%, see Figure 8.1. Varying the heat source temperature, showed the same linear behaviour with efficiency-increasing rate of 1.1%, see Figure 8.2. The LTD Stirling engine showed the highest efficiency. However it works only to a maximum heat source temperature of 160°C, even when changing the working fluid within.

Since this Thesis was limited in time, the heat transfer from the heat source to the working gas was not research focus of the LTD Stirling engine, the results have to be questioned. In fact, the prototype used to simulate the LTD Stirling engine was in the first place developed for solar energy utilization and temperatures around 70°C. Apart from that, today there is no LTD Stirling engine in use for commercial electricity production. Along with that, there is neither long time running experience nor any research of geothermal use. In summary, the LTD Stirling engine shows a large potential for further investigation, but is not ready for commercial use yet.

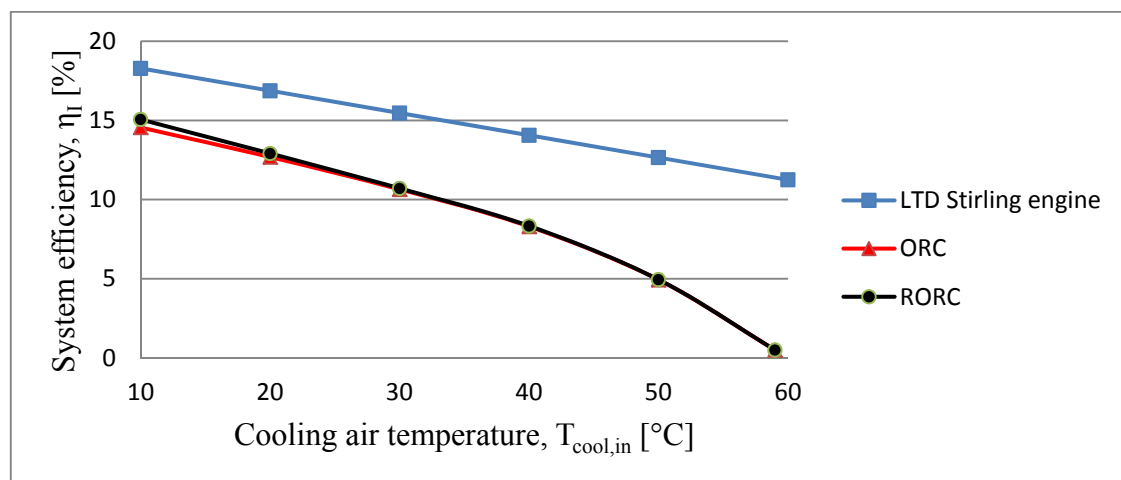


Figure 8.1 System efficiency vs. condenser temperature

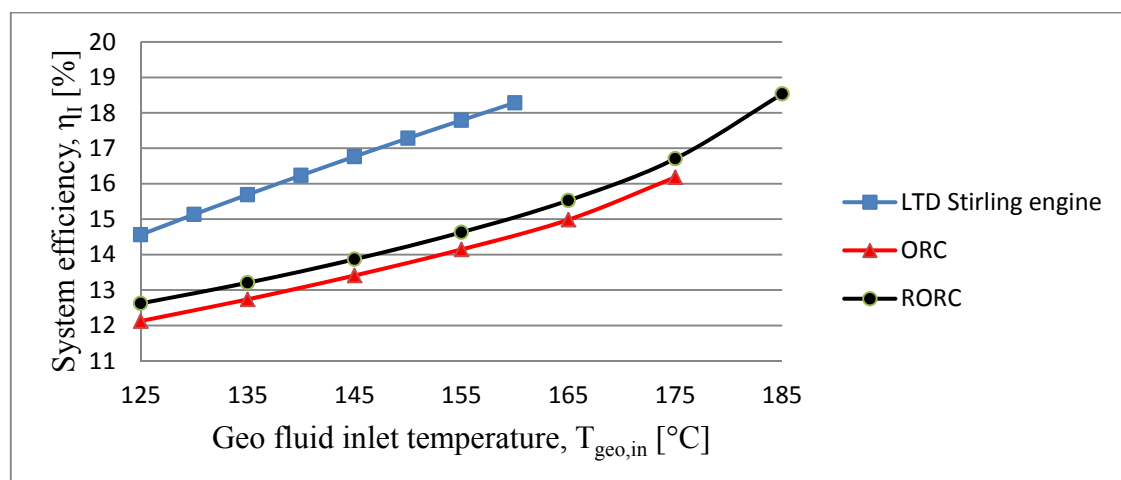


Figure 8.2 System efficiency vs. geo inlet temperature

8.4 Economics

The feed in tariff for electricity varies in Europe from country to country. The profit for each low temperature electricity production technology depends on the following factors:

- The feed in tariff
- The heat source temperature
- The constant geothermal mass flow
- The average constant cooling air temperature
- The yearly operation time

The detailed values are listed in Appendix 3 and in chapter 6. The economic evaluation is shown from

Figure 6.1 to Figure 6.3. In the evaluation are no costs included, neither for the heat, nor for any equipment of the plant.

8.5 Geotermica

In the technical part of the Geotermica case analysis only the ORC and RORC were analysed. The LTD Stirling did not take part during this analysis and the economic analysis for the Geotermica case. The reasons were discussed earlier in this chapter. Based on the weather data from the Aeolian Islands, the expected temperature and flow of the geothermal well, the ORC and RORC have efficiency of 13.4% and 14.2 % respectively. With these efficiencies, they produce roughly 36 GWh and 42 GWh respectively per year.

The costs for the geothermal power plant are composed of exploration and drilling costs and of the plant equipment. Exploration and drilling costs are the lion's share of the costs with 30 Mio. €. With 10.2 Mio. € RORC plant is 1.3 Mio. € more expensive than ORC plant. But with a higher annual electricity production, the procurement costs are paid off for the whole RORC plant in 6.4 years. Compared with the expected ORC plant, the payback time is 0.8 years shorter.

However, the costs were evaluated for a feed in tariff of 15 cent/kWh, but with rising prices for electricity, due to the 20-20-20 targets, probably this feed in tariff is under-priced.

9 Conclusions

Different low temperature electricity production cycles were identified during a literature review for further use in a geothermal power station. Followed by an analysis with set system boundaries, such as heat and cooling source, the systems were compared to each other. This was accomplished with the simulation tool Aspen + and with thermodynamic equations in excel. After that, the cycles have been analysed economically in general. Finally, the geothermal power station for Geotermica has been simulated and calculated. Summarized, the main conclusions from this work are:

- The RORC has been identified to be the most efficient cycle with regards to technical and economic considerations.
- The working fluid has a key influence on the efficiency.
- R245fa has been identified as the most efficient working media. For higher heat source temperature over 185°C, another working fluid like N-pentane should be considered.
- The LTD Stirling engine shows promising results, but is not yet ready for geothermal utilization.
- The Geotermica analysis showed, that the costs for the geothermal power plant make only a small share of the total costs. Therefore a RORC plant with more than one pre-heating stage should be considered
- During this work, the researched power cycles have not been improved, nor experimental validated.

Further work:

- Further investigations should focus on the materials being used, the configuration and number of pistons within the LTD Stirling engine.
- How many pre-heating stages in the RORC are still economical?

10 References

- Alessandro, Franco (2009): Optimal design of binary cycle power plants for water-dominated, medium-temperature geothermal fields [Article] // *Geothermics* 38 (2009) 379-391
- Angelino, G. (2002): Experimental investigation on the thermal stability of some new zero ODP refrigerants [Article] // *International Journal of Refrigeration* 26 (2003) 51-58
- Brown, K. and Dunstall, M. (2000): Silica scaling under controlled hydrodynamic conditions [Article] // *Proceedings World Geothermal Congress 2000, Kyushu-Tohoku, Japan*, pp. 3039-3044
- Chen, D. (2003): Untersuchungen zur Optimierung eines solaren Niedertemperatur-Stirlingmotors
- European Commission (2010): Communication from the Commission, Europe 2020 [Article] // http://europa.eu/press_room/pdf/complet_en_barroso___007_-_europe_2020_-_en_version.pdf
- European Commission (2011) [Online]
http://ec.europa.eu/research/energy/eu/research/geothermal/background/index_en.htm
- European Geothermal Energy Council, (2009): Geothermal Electricity and Combined Heat & Power [Brochure] // <http://www.egec.org/>
- Fridleifsson, I. B. (2001), Geothermal energy for the benefit of the people [Article] // *Renewable and Sustainable Energy Reviews*, 2001 - Elsevier
- Gourdon, M. and Vamling, L. (2011), Selection of working fluids for heat pumps and chillers [Article] // *Heat & Power Technology*, Department of Energy and Environment, Chalmers University of Technology
- Häßler et al. (1997), Darstellung kombinierter thermodynamischer Prozesse // *VGB KWT* 77
- He, Y. (2011), A Vapor injector-based novel regenerative organic Rankine cycle // [Article] *Applied Thermal Engineering* 31 (2011) 1238 -1243
- Ikegami, Y. (2007), The Performance of the Kalina Cycle System 11 (KCS-11) With Low-Temperature Heat Sources [Article] // *Journal of Energy Resources Technology*, September 2007, Vol. 129 / 243
- Jaya, M. S. (2010): Temperature dependence of seismic properties in geothermal rocks at reservoir conditions [Article] // *Geothermics* 39 (2010) 115-123
- Kongtragool B. (2006): Performance of low-temperature differential Stirling engines [Article] // *Renewable Energy* 32 (2007) 547-566
- Kongtragool B. (2002): A review of solar-powered Stirling engines and low temperature differential Stirling engines [Article] // *Renewable and Sustainable Energy Reviews* 7 (2003) 131-154
- Kosmadakis, G. (2008): Comparative thermodynamic study of refrigerants to select the best for use in the high-temperature stage of a two-stage organic Rankine cycle for RO desalination [Article] // *Desalination* 243 (2009) 74-94

Ibrahim, O.M. and Klein, S.A. (1995): Absorption power cycles [Article] // Pergamon 0360-5442(95) 00083-6

Bombarda, P. and Invernizzi, C.M. and Pietra, C. (2010): Heat recovery from Diesel engines: A thermodynamic comparison between Kalina and ORC cycles [Article] // Applied Thermal Engineering 30 (2010) 212-219

Renewable Energy World, (2011) [Online]. - Geothermal feed in tariffs worldwide - <http://www.renewableenergyworld.com/rea/news/article/2011/06/geothermal-feed-in-tariffs-worldwide>

Sinnot, R. & Towler G. (2009) Chemical Engineering Design Elsevier Ltd.

Schwab, A. (2006) Elektroenergiesystem – Erzeugung, Transport, Übertragung und Verteilung elektrischer Energie, Springer Verlag Berlin Heidelberg

Turboden (2011), ORC advantages, <http://www.turboden.eu/en/rankine/rankine-advantages.php>

Wagner, W. and Pruss, A., 1995: "The IAPWS Formulation 1995 for the Thermodynamic Properties of Ordinary Water Substance for General and Scientific Use,"

Walpita, SH. (1983): Development of the solar receiver for a small Stirling engine. In: Special study project report no. ET-83-1. Bangkok: Asian Institute of Technology

Wiemer, H. J. (2009), Thermodynamische Untersuchung zur effizienten Stromerzeugung geothermischer Energie // [Article] "Der Geothermiekongress 2009"

Worek, W. M. And Golubovic M., (2007): The Performance of the Kalina Cycle System 11 (KCS-11) With Low-Temperature Heat Sources [Article] // Journal of Energy Resources Technology, Vol 129 / 247

Yari, M. (2010): Exergetic analysis of various types of geothermal power plants [Article], Renewable Energy 35 (2010) 112-121

Appendix 1

Geo fluid temperature, $T_{\text{geo, in}}$ [°C]	Pressure ratio, p_3/p_4 [bar/bar]			System efficiency, η_I [%]			Carnot-Factor, η_{CF} [%]			Carnot efficiency, η_{Carnot} [%]
	R245fa	R601	H ₂ O	R245fa	R601	H ₂ O	R245fa	R601	H ₂ O	
125	6.3	3.1	2.6	12.8	8.3	5.1	44.4	28.7	17.5	28.9
135	7.1	3.3	2.9	13.5	9.2	5.6	44.2	30.0	18.4	30.6
145	8.2	3.7	3.2	14.3	9.8	6.2	44.4	30.3	19.3	32.3
155	9.6	4.1	3.6	15.2	10.4	6.8	45.0	30.8	20.0	33.9
165	11.8	4.6	3.9	16.3	11.2	7.3	46.1	31.6	20.8	35.4
175	17.2	5.2	4.3	18.2	12.0	7.9	49.3	32.5	21.5	36.8
185		6.1	4.8		12.9	8.4		33.7	22.1	38.2
195		7.3	5.2		13.9	9.0		35.2	22.7	39.5
205		9.0	5.7		15.0	9.5		36.9	23.4	40.8
215		11.8	6.3		16.4	10.1		39.1	23.9	42.0
225		18.5	6.8		18.5	10.6		42.9	24.5	43.2

Appendix 2

Summer		ORC		RORC	
	Unit	Well temperature	Reinjection temperature	Well temperature	Reinjection temperature
Geofluid	°C	150	100	150	100
Cooling air	°C	In	Out	In	Out
		23	33	23	33
System efficiency, η_I	%	12.7		13.3	
Carnot efficiency, η_{carnot}	%	30		30	
Carnot-Factor, η_{CF}	%	42.3		44.3	

Winter		ORC		RORC	
	Unit	Well temperature	Reinjection temperature	Well temperature	Reinjection temperature
Geofluid	°C	150	100	150	100
Cooling air	°C	In	Out	In	Out
		23	33	23	33
System efficiency, η_I	%	14.1		14.9	
Carnot efficiency, η_{carnot}	%	31.9		31.9	
Carnot-Factor, η_{CF}	%	44.2		46.7	

Appendix 3

Summer			
	Month	max. Temperature in °C	min. Temperature in °C
	April	13.5	2.8
	May	18	6.6
	June	21.3	10
	July	23.2	12.1
	August	22.7	11.4
	September	19.6	8.4
	Average	16.45	7.2
<hr/>			
	Total average	14.1	

Climate data for central Europe (Munich) during summer

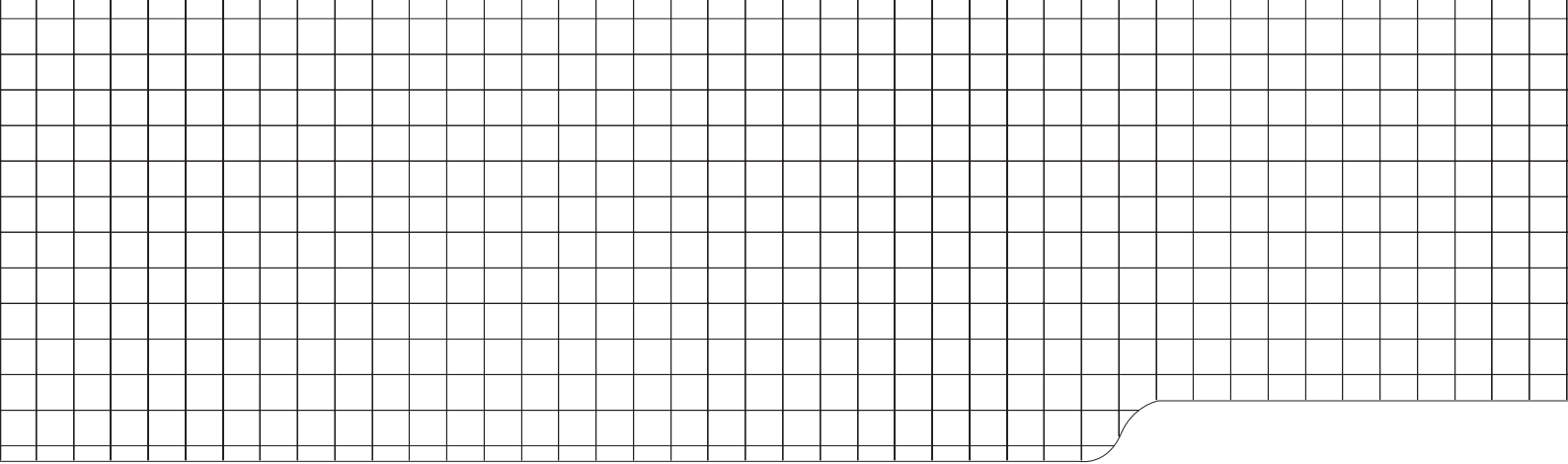
Winter			
	Month	max. Temperature in °C	min. Temperature in °C
	October	13.3	3.7
	November	6.6	-0.1
	December	2.3	-3.8
	January	1.4	-5.6
	February	3.4	-5.1
	March	8.7	-1.5
	Average	4.5	-1.8
<hr/>			
	Total average	1.9	

Climate data for central Europe (Munich) during winter

Appendix 4

Typical factors for estimation of project fixed capital cost	
Item	Process type fluid
Major equipment, total purchase cost	C_e
f_{er} Equipment erection	0.3
f_p Piping	0.8
f_i Instrumentation and control	0.3
f_{el} Electrical	0.2
f_c Civil	0.3
f_s Structures and buildings	0.2
f_l Lagging and paint	0.1
f_m material factor Stainless steel 304 /316	1.3
ISBL cost, $C = \Sigma C_e \times$	3.3
Offsite (OS)	0.3
Design and Engineering (D&E)	0.3
Contingency (X)	0.1

Typical factors for estimation of project fixed capital cost, (Chemical Engineering Design, 2009)



CHALMERS UNIVERSITY OF TECHNOLOGY
SE 412 96 Gothenburg, Sweden
Phone: + 46 - (0)31 772 10 00
Web: www.chalmers.se